Received: 13 September 2024 | Revised: 1 January 2025 | Accepted: 3 February 2025

DOI: 10.1111/jne.70007

ORIGINAL ARTICLE

Journal of Neuroendocrinology WILEY

Kisspeptin fiber and receptor distribution analysis suggests its potential role in central sensorial processing and behavioral state control

Limei Zhang[1,2] | Vito Salvador Hernández[1,2] | Mario Alberto Zetter[1,3] | Oscar Rene Hernández-Pérez[1] | Rafael Hernández-González[4] | Ignacio Camacho-Arroyo[5] | Lee E. Eiden[2] | Robert P. Millar[1,6,7]

[1]Department of Physiology, School of Medicine, National Autonomous University of Mexico, Mexico City, Mexico

[2]Section on Molecular Neuroscience, NIMH-IRP, NIH, Bethesda, Maryland, USA

[3]Department of Medicine and Health, University of La Salle, Mexico City, Mexico

[4]Vivarium, School of Medicine, National Autonomous University of Mexico, Mexico City, Mexico

[5]Research Unit in Human Reproduction, National Institute of Perinatology-Faculty of Chemistry, National Autonomous University of Mexico, Mexico City, Mexico

[6]Centre for Neuroendocrinology, University of Pretoria, Pretoria, South Africa

[7]Department of Integrative Biomedical Sciences, Institute of Infectious Disease and Molecular Medicine, University of Cape Town, Cape Town, South Africa

Correspondence
Limei Zhang and Vito Salvador Hernández, Department of Physiology, School of Medicine, National Autonomous University of Mexico, Av. Universidad 3000, Mexico City, CDMX, 04510, Mexico.
Email: limei@unam.mx and vitohdez@unam.mx

Lee E. Eiden, Section on Molecular Neuroscience, National Institute of Mental Health, NIH, NIHBC 49 CONVENT DR Bethesda, MD 20892, USA.
Email: eidenl@mail.nih.gov

Funding information
La Secretaría de Ciencia, Humanidades, Tecnología e Innovación (Secihti) of Mexico, Grant/Award Number: CF-2023-G-243; Universidad Nacional Autónoma de México, Grant/Award Number: IG-200121; National Institute of Mental Health, Grant/Award Number: MH002386

Abstract

Kisspeptin (KP) signaling in the brain is defined by the anatomical distribution of KP-producing neurons, their fibers, receptors, and connectivity. Technological advances have prompted a re-evaluation of these chemoanatomical aspects, originally studied in the early years after the discovery of KP and its receptor *Kiss1r*. Previously, we characterized (Hernández et al. bioRxiv 2024) seven KP neuronal populations in the mouse brain at the mRNA level, including two novel populations, and examined their response to gonadectomy. In this study, we mapped KP fiber distribution in rats and mice using immunohistochemistry under intact as well as short- and long-term post-gonadectomy conditions. *Kiss1r* mRNA expression was examined via RNAscope, in relation to vesicular GABA transporter (*Slc32a1*) in whole mouse brain, and to KP and vesicular glutamate transporter 2 (*Slc17a6*), *Kiss1*, and *Slc32a1* in hypothalamic RP3V and arcuate regions. We identified KP fibers in 118 brain regions, primarily in extra-hypothalamic areas associated with sensorial processing and behavioral state control. KP-immunoreactive fiber density and distribution were largely unchanged by gonadectomy. *Kiss1r* was expressed prominently in sensorial and state control regions such as the septal nuclei, the suprachiasmatic nucleus, locus coeruleus, hippocampal layers, thalamic nuclei, and cerebellar structures. Co-expression of *Kiss1r* and *Kiss1* was

Limei Zhang and Vito S. Hernández share first authorship.

observed in hypothalamic neurons, suggesting both autocrine and paracrine KP signaling mechanisms. These findings enhance our understanding of KP signaling beyond reproductive functions, particularly in sensorial processing and behavioral state regulation. This study opens new avenues for investigating KP's role in controlling complex physiological processes, including those unrelated to reproduction.

KEYWORDS
autocrine, behavior state system, extrahypothalamic kisspeptin signaling, Kiss1r, sensorial-motor circuits

1 | INTRODUCTION

Kisspeptin (KP) is a neuropeptide encoded by the *Kiss1* gene, initially known as metastin, and identified for its activity in inhibiting cancer metastasis.[1,2] It is now well recognized as a critical regulator of the mammalian reproductive system, playing a pivotal role in the activation of the hypothalamo-pituitary-gonadal (HPG) axis by stimulating the release of gonadotropin-releasing hormone (GnRH).[3,4] Beyond its reproductive functions, KP is increasingly implicated in a variety of physiological processes, including the regulation of emotions and cognitive functions,[5] especially, although not limited to, those involved in sexual behavior.[6] For instance, kisspeptin receptors are expressed in the amygdala and hippocampus, critical regions for emotional processing, and have been associated with both anxiolytic and anxiogenic effects as well as the modulation of stress[7–9] and fear responses.[10–12] Additionally, KP has been implicated in cognitive functions such as learning and memory, potentially through its actions within the hippocampus and prefrontal cortex.[13] Functional imaging has revealed enhanced limbic activity in response to sexual stimuli, and increased ratings for mood, drive, and reward, after kisspeptin infusion in male human subjects.[14] Thus, KP is likely to play a multifaceted role in brain function, beyond the control of the HPG axis.

In a recent study in mice, our group reported a comprehensive KP cell population description and molecular signature characterization within the excitatory/inhibitory (glutamatergic-GABAergic) context throughout the mouse brain, using a sensitive dual and multiple channel in situ hybridization method. We described chemotypes of seven distinct KP populations: four of them within the hypothalamus and three of them as extrahypothalamic populations. The KP cell groups located in the ventral division of the premammillary nucleus of the hypothalamus and the nucleus of the tractus solitarii in the brain stem are new additions to the literature. Their up- and down-regulation by short-term gonadectomy (GNX) was also reported quantitatively.[1] These results prompted us to extend the study by focusing on kisspeptin immunopositive fiber distribution in both rats and mice, and on rodent KP receptor (*Kiss1r*) distribution using the RNAscope method.

There had been comprehensive anatomical studies on KP neuronal populations and fiber distributions in the brain of diverse animal species in the literature of the first decade after the discovery of KP, albeit hypothalamic, rather than extrahypothalamic regions, were the main focus of those studies due to the role of KP in HPG axis regulation.[13,15–19] However, KP may also regulate sexual behavior, in addition to reproductive endocrinology, within the mammalian brain.[6] Due to the emerging evidence for kisspeptin function beyond its well-documented role in orchestration of GnRH secretion in the hypothalamus, more comprehensive data on the distribution of kisspeptin cell bodies and nerve fibers throughout the brain are needed. In particular, some data have been questioned as potentially unreliable, due to possible adventitious cross-reactivity with other RFamide-peptides.[17] We have used a KP antibody with well-documented authenticity and lack of cross-reactivity, and applied state-of-the-art tissue preparation and staining methods[20] in this study. By providing a reliable and comprehensive description of the distribution of KP cell bodies and fibers throughout the brain, we aim to contribute to a better understanding of the possible role(s) of KP first messenger function relevant to both reproductive and non-reproductive behavior. We report here 118 brain regions that contain KP fibers and terminals, with most of them located in extra-hypothalamic regions closely involved in central sensorial processing and behavioral state control.[21–26] KP fiber density was similar in long-term (1 year) gonadectomized compared with intact male or female mice.

The kisspeptin receptor (Kiss1R), belonging to the class A peptide-GPCR family, was first identified in rat in 1999 as an orphan receptor previously called Gpr54.[27] Kiss1R is a metabotropic receptor primarily coupled to $G_{q/11}$, and its inactivation has been associated with hypogonadism.[28] After KP binds its receptor, phospholipase C (PLC) is activated and hydrolyzes phosphatidylinositol 4,5-bisphosphate (PIP2) to produce diacylglycerol (DAG) and inositol 1,4,5-trisphosphate (IP3) with a rise in Ca^{++} mobilized from intracellular stores and the activation of protein kinase C (PKC).[29,30] In a recent study, KISS1R activation of the $G_{i/o}$ pathway was also demonstrated alongside its primary G_q pathway.[31] There have been few reports on Kiss1R expression in the CNS[28,29,32,33] and a comprehensive description, especially Kiss1R co-expression within the context of excitatory and inhibitory neurotransmission, is lacking. In this study, we used the RNAscope dual and multiplex in situ hybridization method to map the *Kiss1r* expression throughout the mouse brain. *Kiss1r* was prominently expressed in sensory processing and brain state control regions, such as the main and accessory olfactory bulbs, septal nuclei, tuberomammillary nuclei, the suprachiasmatic nucleus, the locus coeruleus, the hippocampal pyramidal and granule cell layers, the thalamic nuclei,

and the cerebellar granule cell layer, as well as the interposed nucleus. *Kiss1r* was also co-expressed in *Kiss1*-expressing hypothalamic neurons and neighboring cells, suggesting the KP system uses autocrine and paracrine mechanisms. Data from this study provide new anatomical features of the KP system for further hypothesis generation and testing of the role of KP beyond HPG axis regulation.

2 | MATERIALS AND METHODS

2.1 | Animals

Wistar rats ($N = 12$, male = 6, female = 6) and C57BL/6 mice ($N = 30$, male = 15, female = 15) were obtained from the local animal vivarium and housed three per cage under controlled temperature and illumination (12 h/12 h) with water and food ad libitum. Mice subjected to gonadectomy were singly housed for recovery for 1 week after surgery and then returned to their home cages. All animal procedures were approved by the local research ethics supervision commissions (license number CIEFM-079-2020, UNAM and NIMH/ACUC approval LCMR-08).

To evaluate the effect of gonadectomy on the expression of kisspeptin throughout the brain in male and female mice, we compared the KP immunoactivity of 24 mice distributed in the following experimental groups:

For RNAscope in situ hybridization (ISH) experiments, we used three male and three female mice of 3 months of age. Vaginal cytology was performed in female mice to assess the estrous cycle. Brains were collected during the proestrus stage associated with a high level of estrogen.

Male				Female			
5 month old		15 month old		5 month old		15 month old	
Intact	1 month ORX	Intact	12 month ORX	Intact	1 month OVX	Intact	12 month OVX
$n = 3$	$n = 3$	$n = 3$	$n = 3$	$n = 3$	$n = 3$	$n = 3$	$n = 3$

2.2 | Gonadectomy

2.2.1 | Mouse ovariectomy (OVX)

A dorsal approach to remove the ovaries was used.[34] Briefly, animals were anaesthetized with ketamine 90 mg/kg + xylazine 20 mg/kg i.p. Under anesthesia, animals were placed in ventral recumbency, and a 3 cm/side square region centered over the third lumbar vertebra was shaved and disinfected with povidone and 70% alcohol. A sterile fenestrate drape was placed over the area. A midline dorsal incision ~1 cm long was made in the skin at the level of the bottom of the rib cage. The incision was moved laterally to cut the right and left abdominal walls. After cutting the wall (oblique and transverse abdominal muscles), blunt dissection through the body wall with mosquito hemostats was performed. Forceps were gently and carefully introduced to retrieve and exteriorize the ovary. The ovarian vessels and ligament were ligated with 4-0 synthetic absorbable sutures, and the ovaries were excised. The incision was closed with a 4-0 synthetic, monofilament, and absorbable suture. The skin incision was closed with a subcuticular suture.

2.2.2 | Mouse orchiectomy (ORX)

For the excision of the testicles, we followed a midline incision technique.[35] A 1 cm incision was made in the ventral scrotum, each testis was exposed by blunt dissection and gently pulling it through the incision. The cauda of the epididymis, caput epididymis, vas deferens, and testicular blood vessels were exposed while holding the testicular sac with sterile tooth forceps. A single ligature of 4-0 synthetic absorbable suture around the vas deferens and blood vessels was made before excision and gentle removal of the testis. The remaining contents were replaced in each one of the testicular sacs. The skin incision was closed with a subcuticular suture.

2.3 | Immunohistochemistry (IHC)

Animals were deeply anaesthetized with sodium pentobarbital (100 mg/kg, i.p.). They were perfused transaortically with 0.9% saline followed by a cold fixative containing 4% paraformaldehyde in 0.1 M sodium phosphate buffer (PB, pH 7.4) plus 15% v/v saturated picric acid for 15 min. Brain tissues were rinsed immediately after the 15 min fixation, until the buffer was colorless. Brains were then sectioned the same day, using a Leica VT 1000S vibratome at 70-μm thickness, in the coronal and parasagittal planes, and the immunohistochemical (IHC) reaction was performed the same day. This procedure yielded a more comprehensive IHC labeling than longer fixation and delayed IHC as previously reported and discussed.[20] One of every three sections was selected, and sections from animals that would be compared (i.e., female control vs. female gonadectomy) were incubated in the same vial. To block the nonspecific antibody binding, sections were incubated for 1 h in a solution consisting of 20% normal donkey serum (NDS) diluted in tris-buffered saline (TBS, pH 7.4) plus 0.3% triton-X (TBST). After the blocking step, sections were incubated for 48 h at 4°C with a polyclonal sheep anti-kisspeptin antibody[36] (GQ2, kindly supplied by Mohammad Ghatei† (†: deceased), Imperial College, London, UK), diluted at a 1:5000 concentration in TBST +

1% NDS. This antibody recognizes kisspeptins 54, 14, 13, and 10 that conserve the C-terminal decapeptide essential for biological activity and shows virtually no cross-reactivity (<0.01%) with other related human RF-amide peptides.[36] After three wash steps, sections were incubated for 24 h with the secondary donkey anti-sheep biotinylated antibody (Cat: 713-065-147, Jackson ImmunoResearch Inc., PA) diluted at a concentration of 1:500 in TBST + 1% NDS. To detect the biotinylated antibody, VECTASTAIN Elite ABC HRP Kit (Cat: PK-6100, Vector Laboratories, Inc., CA) was used, with H_2O_2 and 3,3′-diaminobenzidine as substrates. Finally, sections were mounted on glass slides, dehydrated, dipped in xylene, and cover-slipped using Permount mounting medium.

2.4 | Anatomical assessment of kisspeptin innervation density and comparison between control and gonadectomized animals

To assess the projection patterns of kisspeptin immunopositive fibers throughout the brain, four researchers independently examined the slides under a light microscope after identifying the regions based on the Paxinos rat & mouse brain atlases.[37,38] Scores of "+" (sparse, main axons passing, without branching or axon terminals); "++," scattered, some branching; "+++," moderate, abundant branching and axon terminals; "++++," intense, extensive branching and intense axon terminals, with confluent fibers such that it was difficult to see a separation between them, were reported.

2.5 | Anatomical assessment of *Kiss1r* mRNA expression in the context of *Slc32a1*-expressing neurons throughout the brain using DISH method

We mapped *Kiss1r* expression in the whole mouse brain using the RNAscope dual ISH (DISH) method. The DISH method provides samples suitable for light microscope examination, with the ability to quickly and comprehensively examine sections at multiple magnifications. In contrast to the analysis based on fluorescent confocal images previously taken by a single observer, this capability is crucial for low-magnification orientation, identification of neuroanatomical structures, and detailed examination under high magnification verifiable by multiple independent observers analyzing the same samples.

A second mRNA can be chosen for whole brain mapping when using the DISH reaction. We chose *Slc32a1* (mRNA encoding the vesicular GABA transporter VGAT) as a marker for GABAergic neurons. This was based on the consideration that, according to the Allen Institute transcriptomic database, GABAergic neurons constitute 20%–30% of the total neuronal population in the mouse brain. This percentage is higher in subcortical structures, in which their distribution is rather structure-specific compared with more homogeneous cortical regions, providing more precise registration to distinct cell groups during mapping, and providing anatomical context for inhibitory control within the neural circuits in which kisspeptin signaling is important.

Six C57BL mice, 3 male and 3 female 12–14 weeks old, were deeply anesthetized with sodium pentobarbital (100 mg/kg b.w., i.p.) and decapitated using a small animal guillotine. The brains were then extracted and rapidly frozen in Dry Ice. Fresh-frozen brains were sectioned sagittally into 12 µm thick slices using a Leica CM-1520 cryostat and mounted onto positively charged Superfrost Plus microscope slides (Cat. 22-037-246, Fisher Scientific, Pittsburgh, PA). The detailed methods have been previously described.[1,39,40]

Probes used for the detection of mRNAs in the DISH experiment, custom-designed by Advanced Cell Diagnostics (https://acdbio.com), were VGAT (Mm-*Slc32a1*, channel 1) and kisspeptin receptor (Mm-*Kiss1r*, channel 2). All experimental procedures were carried out in accordance with the manufacturer's protocol. After sectioning, the slides were fixed in chilled 4% paraformaldehyde (Cat. 30525-89-4, Sigma-Aldrich) prepared in phosphate-buffered saline (Cat. M32631, Sigma-Aldrich), dehydrated in ethanol, and treated with hydrogen peroxide for 15 min. They were then treated with protease III for 20 min at room temperature, incubated for 2 h with the probe mixtures, and underwent amplification and detection steps following the manufacturer's guidelines. Finally, the slides were counterstained with hematoxylin in the case of DISH and cover-slipped.

The processed sections were examined using a Nikon Eclipse E600 microscope along with its digital camera for photographic documentation. Sections were subsequently scanned using the ZEISS Axio Scan Z1.

For the semi-quantitative analysis, we first examined sagittal and coronal sections from two male and two female mice under low magnification. Using the Paxinos Mouse Brain Atlas, in conjunction with VGAT mRNA (*Slc32a1*) distribution provided by the Allen Mouse Brain Reference Atlas (https://mouse.brain-map.org/experiment/show/79677349 and https://mouse.brain-map.org/experiment/show/72081554), we pinpointed specific brain structures. Once the brain nucleus was identified, we captured light microscope (LM) micrographs at ×40 magnification (one or several micrographs depending on the size of the nucleus). Total numbers of Nissl-stained nuclei, as well as those co-expressing Kiss1r and Slc32a1 or only Kiss1r, were obtained by pooling the counts from micrographs taken of a given brain nucleus across all subjects. Percentages of co-expression (*Kiss1r* and *Slc32a1*) or only Kiss1r were calculated by dividing the corresponding numbers by the total Nissl-stained nuclei in a given region, which populated the columns in Table 3. A single RNA punctum was considered a positive cell, as we did not have another objective criterion based on pre-existing knowledge, although this single-punctum occurrence is quite rare.

2.6 | Anatomical assessment of *Kiss1r* mRNA expression in the context of *Slc32a1*, *Slc17a6*, and *Kiss1* in hypothalamic RP3V and Arc, and cerebellum, using the multiplex-ISH method

The RNAscope multiplex method offers significant advantages for gene expression analysis. It allows for the simultaneous detection of

multiple RNA targets within a single tissue sample, providing a comprehensive overview of gene expression. This method enhances sensitivity and specificity, ensuring accurate localization and quantification of RNA molecules at a single-cell level. Probes used for the multiplex reaction were: kisspeptin (Mm-Kiss1, channel 1), VGAT (Mm-Slc32a1, channel 4), kisspeptin receptor (Mm-Kiss1r, channel 2) and VGLUT2 (mm-Slc17a6, channel 3). All experimental procedures were carried out in accordance with the manufacturer's protocol. After sectioning, slides from one female and one male mouse were fixed in chilled 4% paraformaldehyde (Cat. 30525-89-4, Sigma-Aldrich) prepared in phosphate-buffered saline (Cat. M32631, Sigma-Aldrich), dehydrated in ethanol, and treated with hydrogen peroxide for 15 min. They were then treated with protease III for 20 min at room temperature, incubated for 2 h with the probe mixtures, and underwent amplification and detection steps following the manufacturer's guide. Multichannel ISH sections were analyzed using the Stellaris Confocal Microscope from Leica Microsystems.

3 | RESULTS AND FOCUSED DISCUSSION

3.1 | Regional distribution of kisspeptin-expressing fibers and neurons in the mouse and rat brain

A review of the literature revealed only one prior anatomical mapping study with comparable comprehensiveness in identifying KP-ir in the rat brain. In that study, the authors used an antibody produced by Phoenix Pharmaceuticals,[41] which has been noted as potentially cross-reactive with other RFamide-related peptides.[17] For comparative purposes, we included the data reported by Brailoiu et al.[41] in rat, using the Phoenix Pharmaceuticals antibody anti-metastin (MT), in Table 1, highlighting them in blue. All the regions reported in this earlier study were replicated in our experiments, suggesting that the significance of the earlier report may have been underestimated. On the other hand, we identified numerous additional regions containing KP-expressing fibers, likely reflecting increased sensitivity and a more comprehensive examination in our study. Our conclusions were drawn from 36 brains in serial sections of one of each three sections, each 60 µm thick, cut in both coronal and sagittal planes throughout the brain.

The rat brain, particularly in telencephalic regions (*vide infra*), exhibited stronger immunohistochemical labeling for KP than the mouse brain. However, quantitative conclusions cannot be drawn confidently due to variability among experimental subjects and immunoreactions. Sex differences in the distribution of cells or fibers were inconsistent among experimental subjects, even under identical experimental procedures. For example, within a given region, some reactions were stronger than others, and these differences were not consistently associated with sex or treatment of the subjects. Various unknown factors may have influenced these observations. It is important to note that KP expression may be up- or down-regulated in individual animals due to their physiological regulation, affecting the presence or absence of peptide vesicles at a given location at the time of perfusion-fixation. Specifically, a kisspeptinergic cell (referring to a neuron that can synthesize KP and transport it to its axon or dendrite) can only be detected with KP-IHC if the segment is filled with peptidergic vesicles at the moment of fixation. However, determining these factors falls outside the objective of our study, which aims to qualitatively determine the KP signaling beyond reproductive functions, especially in the brain regions mediating sensory and behavioral states. Based on these observations and rationale, we pooled data from male and female subjects for Table 1 and Figures 1–3, while separating the observations by rodent species (i.e., mouse in Figures 1 and 2 vs. rat in Figure 3) to depict the highest possible KP expression in a given region. This scoring reflects the maximum density observed for each region, providing insight into the maximum potential expression of KP in living rodents. In Figure S1, we present examples of KP IHC labeling in young male and female mice, both intact and gonadectomized, to further illustrate this point.

In Figure 1, we show KP immunohistochemical reactivity (-ir) in regions, including anteroventral periventricular nucleus (AVPV) and ventromedial preoptic area (VMPO), where KP functions to regulate GnRH secretion, in comparison with other brain regions, with equally intense KP innervation, that are relevant to regulation of other functions,[22] including median preoptic nucleus (MnPO), septohypothalamic nucleus (SHy), medial septal nucleus (MS, panel A2), lateral septal nucleus (LS), and bed nucleus of stria terminalis (BST, which includes the medioanterior, medioventral and lateroventral divisions, STMA, STMV, and STLV, respectively) (panel A). In panel A3, KP-ir cell bodies can be seen in the periventricular region (black arrows). Numerous KP-ir fibers are densely distributed at the ventricular wall with several endings observed at the ventricular lining within the ependymal cell layer (red arrows), suggesting a humoral-secretory function of KP signaling. Panel B depicts a coronal section around bregma −0.15 mm, where four main conducting fiber systems can be clearly seen, that is, the anterior commissure (ac), the stria medullaris (sm), the stria terminalis (st), and the fornix (f). KP-ir fibers running inside these conducting systems are indicated with red arrows. The dense innervation pattern of KP-ir fibers in the paraventricular anterior nucleus of the thalamus is shown (panel B). In panels C and D we show examples of KP-ir cell bodies and fibers in amygdalar complex. KP-ir fibers can be seen inside the stria terminalis (st), bed nucleus of stria terminalis, intra-amygdalar division (STIA), baso-medial amygdala (BMA), nu. basalis of Meynert (NBM), and medial amygdala (MEA). Interestingly, some fibers within the medial amygdala, postero-dorsal division (MEApd), are observed coming from the stria terminalis, with main axons branching within the MEApd, and possibly originating from the hypothalamus. We observed fibers reaching to amygdala, through the stria terminalis (C1, red arrows). This observation is also supported by the analysis from the Allen Mouse Brain Connectivity Atlas (see Table 1, last two columns entitled "Axons from RP3V viral tracers" and "Axons from Arc viral tracers" and in the Figure S2). Panels E and F show the photomicrographs taken from the hypothalamic tuberal region, where the KP-ir cell bodies are seen in the posterior division of the arcuate nucleus (ArcP) and in premammillary nucleus, ventral division (PMv). KP-ir fibers are observed in other

TABLE 1 Comparison of the distribution of kisspeptin immunoreactive fibers in mouse and rat brain using antibody GQ2 (current study) to earlier reports using metastin MT antibody (Brailoiu et al.[41]).

Structure	Abbr.	irMT cells (rat)	irGQ2 cells rat	irGQ2 cells mouse	irMT fibers (rat)	irGQ2 fiber rat	irGQ2 fiber mouse	Axons from RP3V viral tracers	Axons from Arc viral tracers
Telencephalon									
Cerebral cortex									
Cingular cortex	Cg		–	–		++	+		
Dorsal peduncular cortex	DP		–	–		++	+		
Dorsal tenia tecta	DTT		–	–		++	+	+	
Infralimbic cortex	IL		–	–		++	+		
Prelimbic cortex	PrL		–	–		++	+		
Ventral orbital cortex	VO		–	–		++	+		
Olfactory area									
Anterior olfactory nucleus	AON		–	–		++	+		+
Olfactory tubercle	Tu		–	–		++	+		
Extended amygdala									
Anterior amygdala	AA		–	–		++	+		
Bed nucleus of stria terminalis medioanterior	BSTMA		–	–	++	+++	+++		+
Bed nucleus of stria terminalis medioposterior	BSTMP		–	–	++	+++	+++		+
Bed nucleus of stria terminalis laterodorsal (oval)	BSTLD		–	–	++	+	+	++	
Bed nucleus of stria terminalis lateroventral	BSTLV		–	–	++	+++	+++	++	
Bed nucleus of stria terminalis lateroposterior	BSTLP		–	–	++	+++	+++		
Basolateral amygdala	BLA		–	–	+	+	+		
Basomedial amygdala	BMA		–	–	+	+	+	++	+
Bed nucleus of stria terminalis intra-amygdala division	BSTIA		–	–		++	++		
Central amygdaloid nucleus, lateral	CeL		–	–	+	+	+	–	–
Central amygdaloid nucleus, capsular	CeC		–	–		++	++	–	–
Central amygdaloid nucleus, medial	CeM		–	–	+	++	++	–	–
Cortico-amygdala	CoA		–	–		+	+		+
Medial amygdaloid nucleus, posterodorsal	MePD		+	+		++	++		+
Medial amygdaloid nucleus, posteroventral	MePV		–	–		++	++	+	+
N. lat. olfactory tract	NLOT		–	–		+	+	–	
Stria terminalis	st		–	–		+	+		
Basal ganglia									
Accumbens n., core	AcbC		–	–	+	++	++	+	+
Accumbens n., shell	AcbSh		–	–		+++	++	++	+
Caudate putamen	CPu		–	–	+	+	+		
Globus pallidus	GP		–	–		+	+		
Internal capsule	ic		–	–		+	+		
External capsule	ec		–	–		+	–		

TABLE 1 (Continued)

Structure	Abbr.	irMT cells (rat)	irGQ2 cells rat	irGQ2 cells mouse	irMT fibers (rat)	irGQ2 fiber rat	irGQ2 fiber mouse	Axons from RP3V viral tracers	Axons from Arc viral tracers
Substantia innominata	SI		–	–		+	+	+	
Ventral pallidum	VP		–	–	+	++	++		
Septum									
Lat. septal n. dorsal	LSD		–	–	++	+++	+++	+	
Lat. septal n. int	LSI		–	–	+	+	+		++
Lat. septal n. ventral	LSV		–	–	++	+++	+++	+++	++
Medial septal nucleus	MS		–	–	+	+++	+	+	+
Septo-fimbrial n.	SFi		+	+		+	+	++	
Septo-hippocampal n.	SHi		+	+		+	+		
N. horizontal limb of the diagonal band	HDB		–	–	+	+	+	++	+
N. vertical limb of the diagonal band	VDB		–	–	+/–	+	+	+++	+
Diencephalon									
Hypothalamus									
Anteroventral periventricular n.	AVPe		+++	+++		+++	+++	+++	+++
Rostral periventricular area	RP3V		+++	+++		+++	+++		
Anterior hypothalamic area anterior	AHA		–	–		++	++	++	+++
Anterior hypothalamic area posterior	AHp		+	+	+	++	++		+++
Arcuate nucleus	Arc	+	++	++	+++	+++ +	++++	+++	++++
Dorsal hypothalamic	DH		+	+	+	+	+	+++	
Dorsomedial hypothalamic area	DM	+++	++	++	++	++	++	+++	++
Lat. hypothalamic area	LH		–	–	+	+	+	+	+
Lat. preoptic area	LPO		–	–	+	++	++	+++	
Medial preoptic area	MPA		–	–	+	++	++	+++	++
Medial preoptic n.	MnPO		–	–	+	+++	+++	++++	+++
Parastrial nucleus	PS		–	–	+++	+++	+++		
Paraventricular hypothalamic n.	PVN	+	–	–	+	++	+	+++	+
Paraventricular hypothalamic n. medial magnocellular div	PVNmm		–	–		+++	+++	+++	+
Pa hypothalamic n. lateral magnocellular div.	PVNlm		–	–		+	+	+++	+
Pa hypothalamic n. medial parvocellular div.	PVNmp		–	–		+++	+++	++	
Periventricular hypothalamic n. anterior	PVa		–	–		++	++		+++
Premammillary n. ventral	PMv		+	+		+++	++	+++	+++
Posterior hypothalamic area	PH		–	–	+	+	+	++	++
Retrochiasmatic area	RCh		–	–	+	+	+	++	++
Supraoptic nucleus	SON		–	–	+	++	++	+	
Tuber cinereum area	TC		–	–	+	++	+	++	
Ventral tuberomammillar n.	TMv		–	–		+++	++		+++

(Continues)

TABLE 1 (Continued)

Structure	Abbr.	irMT cells (rat)	irGQ2 cells rat	irGQ2 cells mouse	irMT fibers (rat)	irGQ2 fiber rat	irGQ2 fiber mouse	Axons from RP3V viral tracers	Axons from Arc viral tracers
Ventromedial hypothalamic nucleus	VMH	+	–	–	+	+	+		+
Thalamus									
Anteromedial thalamic nucleus	AM		–	–		++	++		
Central medial thalamic nucleus	CM		–	–	+	+	+	++	
Mediodorsal thalamic nucleus	IMD		–	–	+	+	+		
Paratenial thalamic nucleus	PT		–	–	+	+	+		
Periventricular thalamic nucleus	PVT		–	–	+++	+++ +	++++	++	+
Reuniens thalamic nucleus	Re		–	–	+	+	+		
Rhomboid thalamic nucleus	Rh		–	–	+	+	+		
Submedius thalamic nucleus	SubD		–	–		+	+		
Zona incerta	ZI		–	–	+	+	+		
Epithalamus									
Habenular nucleus	Hb		–	–	++	++	++	+	
Mesencephalon									
Central nucleus of the inferior colliculus	CIC		–	–	+	++	++		
Cuneiform nucleus, dorsal part	CnFD		–	–		++	++		
Dorsal raphe nucleus	DR		–	–	+	++	++		
Deep mesenceph. n.	DpMe		–	–	+	+	+		
Interpeduncular n.	IP		–	–		+	+		
Median raphe n.	MnR		–	–	+	+	+		
Periaqueductal gray, lateral	LPAG		–	–		++	++	++	+
Periaqueductal gray dorsomedial	DMPAG	+/–	–	–	+++	+++	+++	++	+
Substantia nigra	SN		–	–	+	+	+		
Superior colliculus, intermediate and deep gray layer	DpG		–	–	+	+	+		
Supramammillary n.	SuM		–	–	+	+	++		
Ventral tegmental area	VTA		–	–		+	+	+	
Metencephalon and myelencephalon									
Ambiguus nucleus	Amb		–	–	+	+	+		
Area postrema	AP		+	+		+++	+++		
Caudoventrolateral reticular nucleus	CVL	+	–	–	+	++	++		
Dorsomedial tegmental area	DMTg		–	–		+	+		
Gigantocellular reticular nucleus	Gi		–	–	+	++	++		
Intermediate reticular nucleus	IRt		–	–	++	++	++		
Lateral parabrachial nucleus	LPB		–	–	+++	+++ +	++++	+	
Lateral reticular nucleus	LRt	+			++	++	++		
Lateral superior olive	LSO		–	–	++	+	+		
Locus coeruleus	LC		–	–	++	+++	+++	+	
	MVeMC		–	–		++	++		

TABLE 1 (Continued)

Structure	Abbr.	irMT cells (rat)	irGQ2 cells rat	irGQ2 cells mouse	irMT fibers (rat)	irGQ2 fiber rat	irGQ2 fiber mouse	Axons from RP3V viral tracers	Axons from Arc viral tracers
Medial vestibular nucleus, magnocellular part									
Medioventral periolivary nucleus	MVPO		–	–		+++	+++		
Medullary reticular nucleus, dorsal part	MdD		–	–	+	++	++		
Medullary reticular nucleus, ventral part	MdV		–	–	+	+	+		
Nucleus of the solitary tract	Sol	+++	++	++	+++	+++ +	++++		
Parvicellular reticular nucleus	PCRt		–	–		++	++		
Parabrachial pigmented nucleus	PBP		–	–		+	+		
Pontine nuclei	Pn		–	–	+	–	–		
Pontine n, brachium pontis	bpPn		–	–		+	+		
Pontine raphe nucleus	PnR		–	–	+	–	–	+	
Pontine reticular nucleus, caudal part	PnC		–	–	+	+	+	++	
Pontine reticular nucleus, oral part	PnO		–	–	+	+	+	++	
Principal sensorial 5 n. dorsomedial	Pr5DM		–	–		+++ +	++++		
Raphe magnus nucleus	RMg		–	–	+	+	+		
Raphe obscurus nucleus	Rob		–	–	+	+	+		
Raphe pallidus nucleus	RPa		–	–	+	+	+		
Rostroventrolateral reticular nucleus	RVL		–	–	++	++	+		
Rubrospinal tract	rs		–	–	++	++	++		
Spinal trigeminal tract	Sp5	+	–	–	+++	–	–		
Spinal 5, gelatinous layer	Ge5		–	–		+++ +	+		
Superior cerebellar peduncle	scp		–	–		+++	+++		

Note: Distribution of kisspeptin immunoreactive (antibody GQ2) fiber distribution in mouse and rat brain with comparison of metastin, MT antibody, from Brailoiu et al.[40] in blue lettering. Semiquantitative annotations are used here: "–" not observed; "+" (sparse, main axons passing, without branching or axon terminals); "++", scattered, some branching; "+++", moderate, abundant branching and axon terminals; "++++", intense, extensive branching and intense axon terminals, with multiple confluent fibers. Anatomical regions are ordered based on Brailoiu et al.[41] (columns with blue lettering) modified based on Allen Institute Mouse Reference Atlas. For the Brailoiu study, the immunoactivity ratings are: +/–, sparse; +, modest; ++, moderate; +++ intense. Regions of rat brain with higher density of KP fibers than mouse are highlighted with bold lettering. The two columns to the right are from analysis of two *Kiss1*-Cre mice injected with Cre-dependent tracer in the arcuate nucleus (Arc, experiments 232311236 and 232310521) and two in the rostral periventricular region (R3PV, experiments 299247009 and 301989585) from the Allen Mouse Brain Connectivity Atlas (https://connectivity.brain-map.org/).

regions relevant for behavioral state control at this level, such as ventral tuberomammillary nu (VTM), magnocelular tuberomammillary nu. (MT), and dorsal tuberomammillary nu. (DTM), posterior hypothalamus, zona incerta (ZI), and subthalamic nu. (STN) (E). Figure 1E2 shows the third ventricle at the level of Arc posterior where abundant KP-ir fibers extended toward the lumen of the ventricle (also see Figure 1A3, red arrows). In hindbrain, KP-ir cell bodies and dense KP-ir fibers are seen in the solitary tract (sol) nu. (NTS) of mouse medulla (Figure 1G-K). H and I show the dense innervation pattern of KP-ir fibers in pontine nuclei: lateral parabrachial nu. (LPBN) and locus coeruleus (LC), respectively. KP-ir fibers densely innervate the spinal trigeminal tract (Sp5, K) and in the gelatinous layer of Sp5 (Ge5, J). Perisomatic contacts made by KP-ir fibers and cell bodies within the Ge5 are observed (Figure 1J).

In Figure 2, we present chartings of mouse KP cell and fiber distribution in register with a previous study[15] for purposes of comparison. Panels A, B, and C show intense KP innervation of the prefrontal structures, such as cingulate cortex (Cg), dorsal peduncular cortex

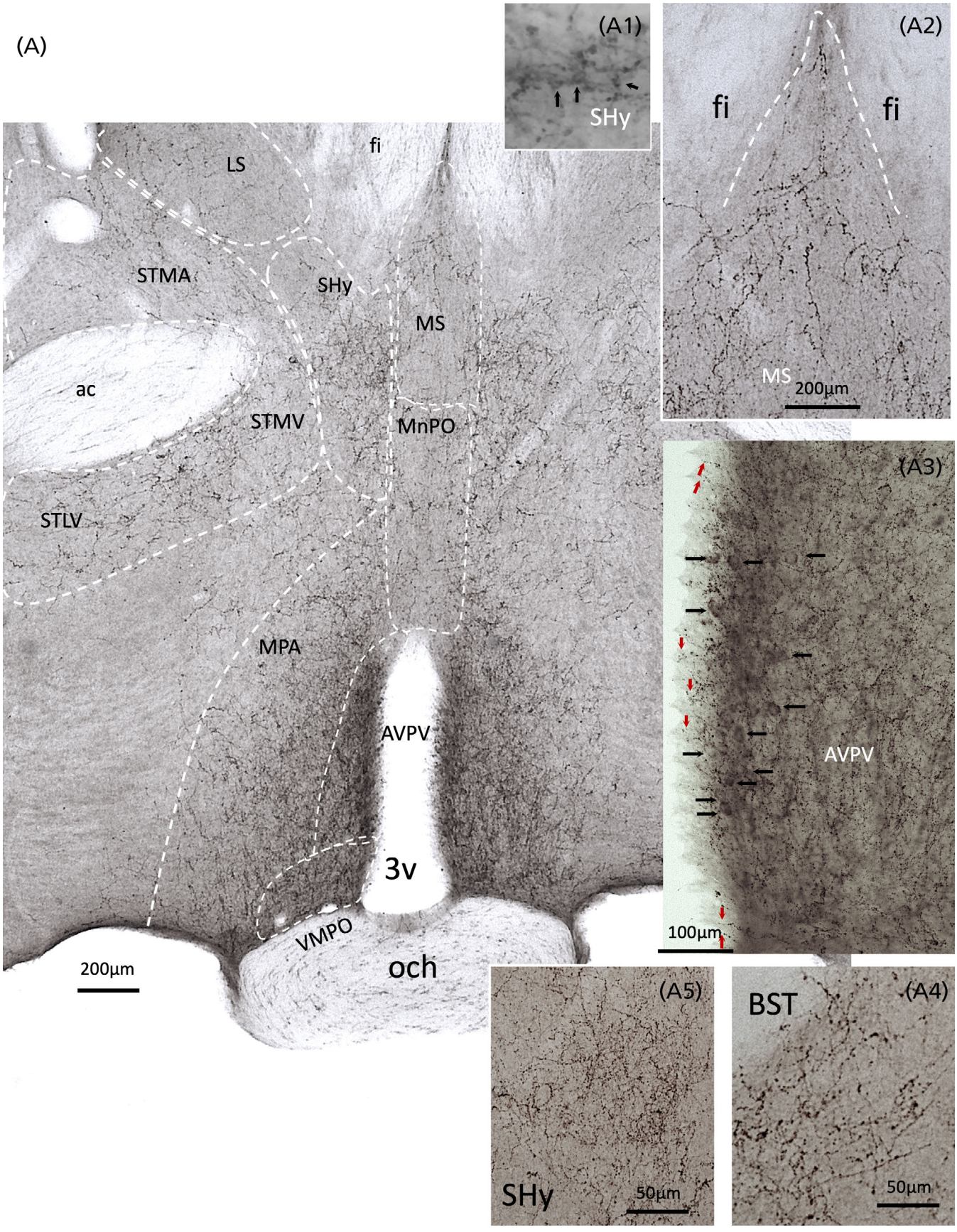

Figure 1 Legend on next page.

(DP), dorsal tenia tecta (DTT), infralimbic cortex (IL), prelimbic cortex (PrL), ventral orbital cortex (VO), nucleus accumbens shell (AcbSh), medial septal nucleus (MS), nucleus of the diagonal band of Broca (NDB), and dorsal division of the lateral septal nucleus (LSd), which were not previously reported. We also observed abundant innervation in thalamic structures such as nucleus reuniens (Re), periventricular anterior nucleus (PVA), and the epithalamic lateral habenula (LHb). In the amygdaloid complex, we observed KP innervation in cortico-amygdala (CoA), nucleus of the lateral olfactory tract (NLOT), medial amygdala (MEA), mainly in the postero-dorsal division (MEApd), basomedial amygdala (BMA), basolateral amygdala (BLA), and nucleus of the stria terminalis, intra-amygdala division (BSTIA) (Figure 2D–G). Midbrain and hindbrain sensorial relay and state control centers, such as the premammillary nucleus (PM), dorsal raphe nucleus (DR), periaqueductal gray (PAG), subthalamic nucleus (STh) parabrachial complex (PBc), locus coeruleus (LC), Koelliker–Fuse nucleus (KF), and nucleus of solitary tract (NTS), all possess KP-ir fibers not reported previously (Figure 2H–L).

Kisspeptin (KP) innervation patterns in rat brain are presented in Figure 3. This figure maps KP-immunoreactive fibers (red lines) and cell bodies (blue dots) across ten septo-temporal levels of the rat brain. We observed a pattern of KP fiber distribution similar to that in the mouse brain, particularly in the hypothalamic regions. However, some qualitative differences were noted in the density and extent of KP innervation (see Table 1 for comparison between column "irGQ2 fiber rat" and column "irGQ2 fiber mouse"). Bold lettering indicates stronger expression in rat than mouse. The differences are especially apparent in the telencephalic and diencephalic regions, where a generally stronger KP expression was observed in rat brain. These regions include the cingulate cortex, dorsal peduncular cortex, dorsal tenia tecta, infralimbic cortex, prelimbic cortex, ventral orbital cortex, olfactory area, anterior olfactory nucleus, olfactory tubercle, extended amygdala, anterior amygdala, and accumbens shell. These differences emphasize the importance of comparative studies to understand the conserved and divergent roles of KP signaling across different species, particularly in non-reproductive functions, where KP signaling may have undergone exaptation to serve other relevant functions for the species in question.[42]

3.2 | Detailed description of regional distribution of KP fibers with an emphasis on sensorial processing and behavioral state control

The distribution of kisspeptin fibers in several regions containing crucial central sensorial relays and behavioral-state control structures[21–26] suggests wider participation of this peptide in other functions besides reproduction and energy balance. In the following sections, we describe these regions in detail.

3.2.1 | Telencephalon

In rodent telencephalon, the most prominent KP fiber-expressing regions are located in the *lateral septal region* in male and female mice and rats. The strongest expression was observed in the dorsal lateral septal nucleus (LSD) (Figures 1A,A2, 2B,D and 3B,C), followed by ventral LS (LSV) (Figures 2C and 3C). LS is involved in the integration of

FIGURE 1 Mouse KP immunoreactive (-ir) fiber distribution in brain regions relevant to regulation of brain state. Panel A shows a low magnification micrograph at coronal plane bregma 0.38 mm[37], where hypothalamic kisspeptinergic regions (containing KP-ir cell bodies), such as the antero-ventral periventricular nucleus (AVPV, A3) and ventromedial preoptic nucleus (VMPO) are located. Regions with high densities of KP innervation, which are relevant for brain state control, such as medial nucleus of preoptic area (MnPO), septo-hypothalamic nucleus (SHy, A1, A5, which also contains KP cell bodies, indicated with black arrows), medial septal nucleus (MS, A2), lateral Septal nu. (LS), bed nucleus of stria terminalis (BST, A4) are shown in high magnification. BST with its subdivisions medio-anterior (STMA), medio-ventral (STMV), and latero-ventral (STLV) are visible in low magnification in panel A. A3 shows the KP-ir in AVPV, where KP-ir neurons are indicated with black arrows and abundant KP-ir fibers innervating the ventricular surface are indicated with red arrows. Panel B, micrograph of a coronal section around bregma −0.15 mm, where four brain main conducting fiber systems, that is, the anterior commissure (ac), the stria medullaris (sm), the stria terminalis (st), and the fornix (f) can be clearly seen. KP-ir fibers running inside these conducting systems are indicated with red arrows. Also, the dense innervation pattern of KP-ir fibers in the paraventricular anterior nucleus of the thalamus (PVA) is shown. Panel C shows a low magnification micrograph of amygdala around the coordinate bregma −1.58 mm in coronal plane. KP-ir fibers can be seen in stria terminalis (st), bed nucleus of stria terminalis, intra-amygdalar division (STIA), baso-medial amygdala (BMA), nu. basalis of Meynert (NBM), and medial amygdala (MEA). Some fibers within the medial amygdala, postero-dorsal division (MEApd), are observed coming from the st, where the main axon entered the MEApd and branched locally (C1, red arrows). Panel D shows a micrograph of MEApd at bregma −2.18 mm. Numerous KP-ir cell bodies are indicated with red arrows. D1 shows a low magnification micrograph of the panel D. Panels E and F, and subpanels, show the microphotographs taken from the hypothalamic tuberal region, where the KP-ir cell bodies are seen in arcuate nucleus (Arc). E and F1 show KP-ir cell bodies in premammillary nucleus, ventral division (PMv, E and E1, F3) and in the dorso-medial hypothalamic region (DMH, F, F1 and F2, black arrows). KP-ir fibers are observed in other regions relevant for behavioral state control at this level, such as ventral tuberomammillar nucleus (VTM), magnocelular tuberomammillar nucleus (MT) and dorsal tuberomammillary nucleus (DTM), posterior hypothalamus (PH), zona incerta (ZI), and subthalamic nu. (STN) (E). E2 shows the third ventricle at the level of Arc, posterior division (ArcP). Abundant KP-ir fibers extended toward the lumen of the ventricle (red arrows, E2). Panel Gs-K are micrographs of samples from parasagittal sections of mouse hindbrain. Panel G and subpanels show the KP-ir cell bodies and dense KP-ir fibers in the solitary tract (sol) nucleus (NTS) of mouse medulla. H and I show the dense innervation pattern of KP-ir fibers in pontine nuclei: Lateral parabrachial nucleus (LPBN) and locus coeruleus (LC), respectively. J and K show the dense KP-ir fibers in the spinal trigeminal tract (Sp5, K) and in the gelatinous layer of Sp5 (Ge5). Note that within the Ge5, the KP-ir fiber make perisomatic contacts with the cell bodies of the Ge5 (J, red arrows).

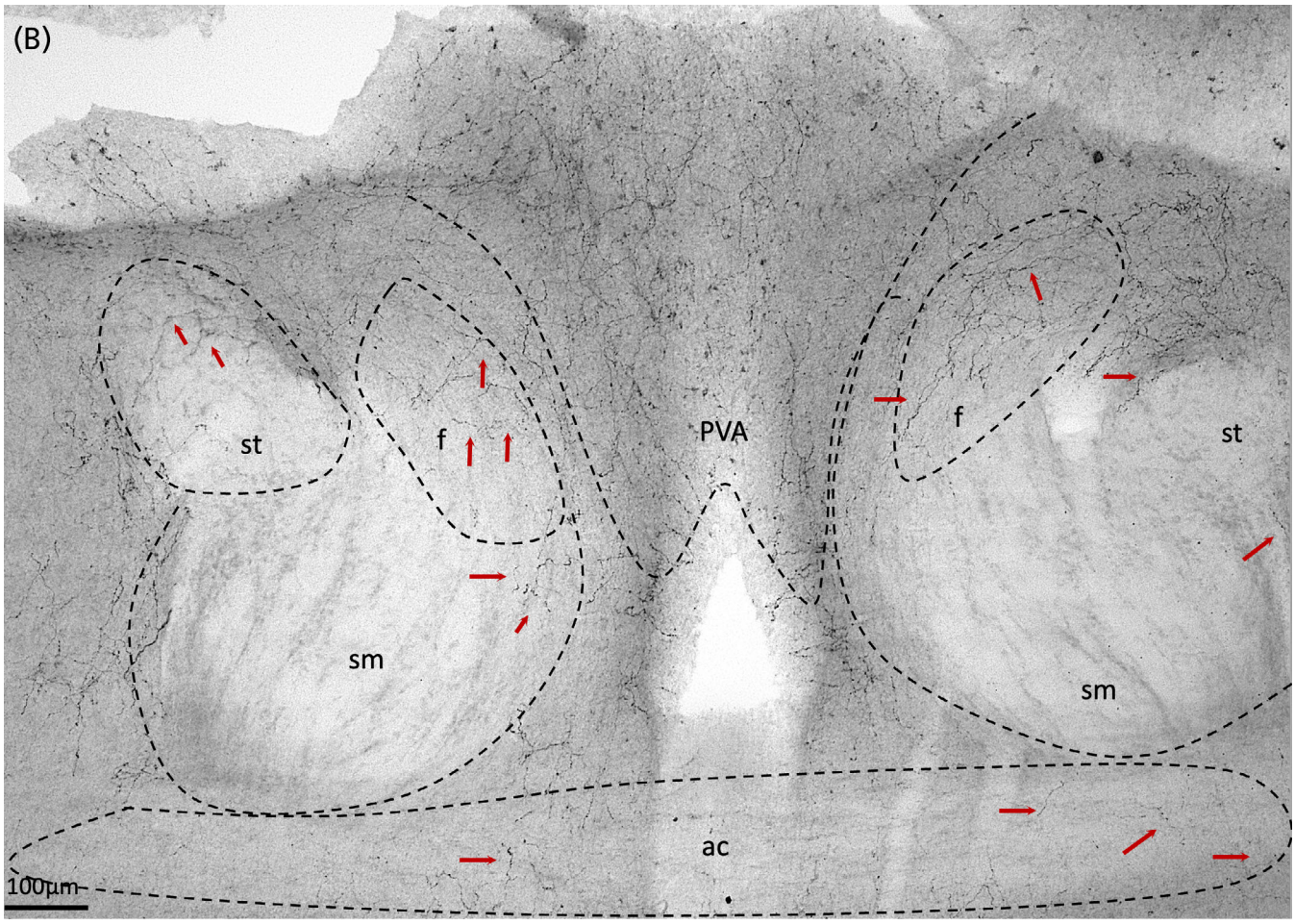

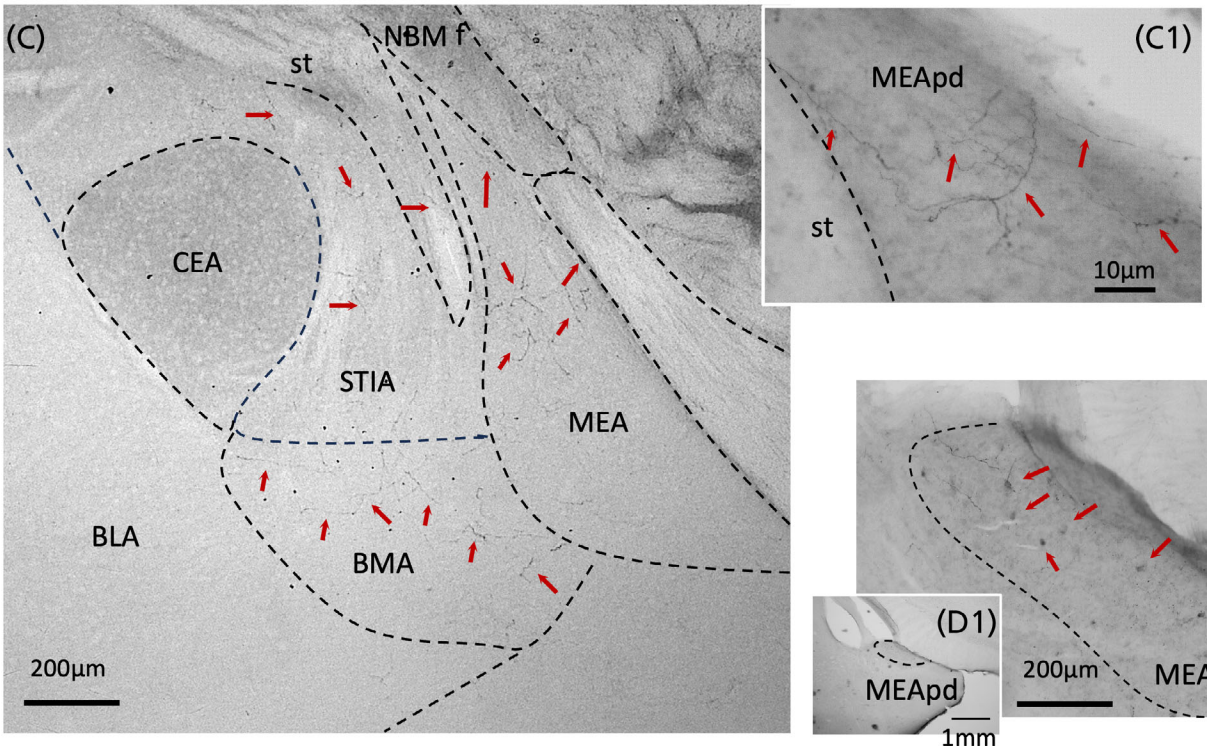

FIGURE 1 (Continued)

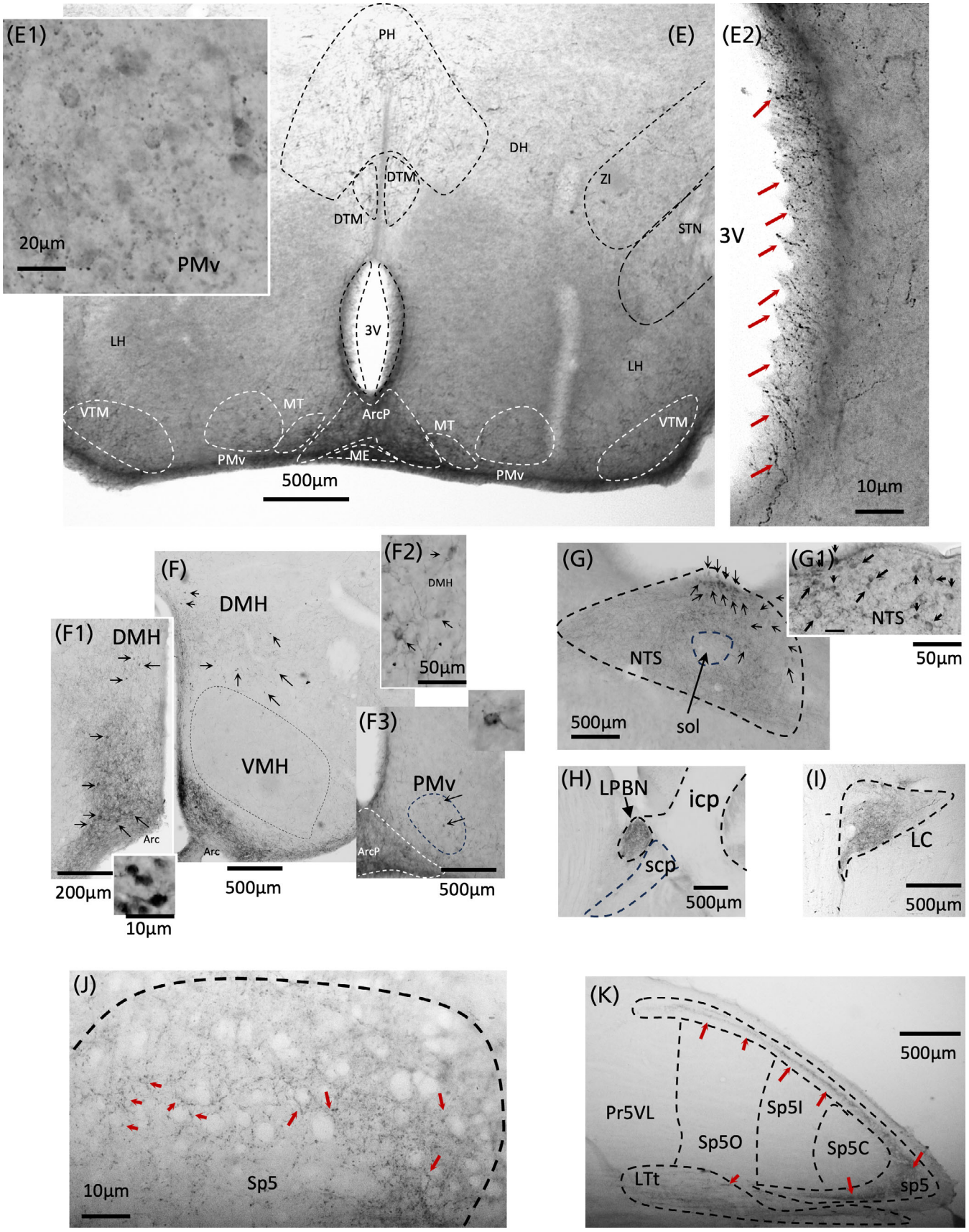

FIGURE 1 (Continued)

sensorial and emotional information and can modulate the activity of other brain regions involved in the regulation of behavioral states, such as the hypothalamus, amygdala, and hippocampus.[43,44] Recent studies have reported the main afferents of the above regions are the subdivisions of the hippocampal formation and the main efferent regions of the LSD are the ventral tegmental area and the supramammillary nucleus, whereas the LSV projects mainly to the medial hypothalamic area and medial preoptic area.[44] Activity of the lateral septum can lead to changes in behavioral state, including increased exploratory behavior, social interactions, and decreased anxiety, particularly in response to social and emotional stimuli. LS is also a key player for arousal and wakefulness, as well as for regulating processes related to mood and motivation through its extensive connections with numerous regions such as the hippocampus, amygdala, hypothalamus, and the mesocorticolimbic dopamine system.[45]

The *medial septum* (MS) also contained scattered and sparse KP innervation in rats and mice (Figures 1A and 2B). This structure is crucially involved in regulating hippocampal oscillations,[46,47] that is, the rhythmic pattern of neuronal activity detected via changes in local field potential, which have been found to be relevant for the encoding of information and supporting processes such as learning and memory.[48] Recent studies have shown that the medial septum acts as a neural hub that regulates theta oscillations and locomotion speed, influencing goal-directed behaviors such as spatial navigation.[49] Other behaviors influenced by the medial septum include sleep, attention, learning and memory, motivation, and emotional processing.[50–52]

Sparse KP fibers were found in the septofimbrial nucleus (Figure 3B), which is an important source of cholinergic inputs to the hippocampus and entorhinal cortex that influence hippocampal plasticity and learning and memory under emotional stimuli; and the septohippocampal (SHi, Figure 2B) nuclei that provide important GABAergic inputs to the hippocampus playing a role in the generation of hippocampal theta oscillation.[53] The above two KPergic regions are described for the first time in this study.

Similar to Brailoiu et al.,[41] we found sparse fibers in the horizontal and vertical limbs of the nucleus of the diagonal band of Broca (NDB) (Figure 2B). The diagonal band of Broca interconnects the amygdala and the septal area and projects particularly to the CA2 subfield of the hippocampus, which is involved in memory retrieval and social functions.[54,55] It contains the second largest cholinergic neuronal population in the brain (after the nucleus basalis of Meynert).[56] It is particularly important in the aging of the brain, since the cholinergic neuronal loss in dementias has been commonly observed in humans, suggesting a possible connection between KP neuromodulation and neurodegeneration-associated cognitive dysfunction.

An interesting finding of this study was the remarkable presence of kisspeptin fibers in the *nucleus accumbens*, in both core and shell divisions (AcbC and AcbSh), with a low density in mice and a moderate density in rats (Table 1; Figures 2A and 3B–D). AcbC receives inputs from the prefrontal cortex, the amygdala, and the ventral tegmental area (VTA), which is a key component of the brain's reward system. The AcbC integrates these inputs to evaluate the salience and value of rewards and helps to regulate motivated behavior. The nucleus accumbens shell is an important brain region involved in the processing of reward-related information and the regulation of motivated behavior, including food intake, drug seeking, and social behavior.[57]

Sparse KP fibers were observed in the caudate putamen (CPu, Figures 2D and 3C), ventral pallidum (VP, Figure 3D), the substantia innominata (SI), and in main fiber pathways such as the internal capsule (ic) and external capsule (ec).

In telencephalic neocortical regions, we found sparse fibers distributed through the dorsal tenia tecta (DTT) and the dorsal peduncular (DP), prelimbic (PrL), infralimbic (IL), and cingular (Cg) cortices, regions not reported in previous studies. The observed fibers were mainly located in layers 2/3, and no differences between species were observed (Table 1; Figures 2A and 3B). The prelimbic (PrL), infralimbic (IL), and cingulate (Cg) cortices have been classically considered to be involved in integrating the role of context into the expression of fear- or reward-induced behaviors.[58–60] The DTT and the DP have been classically involved in olfactory information processing, and recently these two structures have been shown to send inputs with information related to psychosocial stress to the dorsomedial hypothalamus, where a cardiovascular and thermogenic sympathetic stress response can be integrated.[61] In other areas classically related to the processing of olfactory information, such as the ventral and ventroposterior regions of the anterior olfactory nucleus (AOV and AOVP) and the olfactory tubercle (Tu), we found sparse fibers only in the rat (Table 1; Figure 3B–D).

In the amygdalar complex, we confirmed the KP-ir cell population mainly confined within the medial amygdala's postero-dorsal division (MePD) which has been reported already elsewhere[62,63] (Table 1; Figures 1C,D, 2F,G, and 3F,G). The ISH study in gonadally intact rats and mice showed that *Kiss1* levels were higher in males than females and fluctuated with the estrous cycle, peaking at proestrus in rats[64] suggesting its potential influence on reproductive and broader brain functions. Kisspeptin-immunolabeled neurons in the MePD and an axon terminal process were observed to innervate the adjacent nucleus of the stria terminalis intra-amygdaloid division and the stria terminalis. Also, we observed KP-expressing cell bodies in the septohippocampal (SHi) and septo-fimbrial (SFi) regions surrounding the anterior commissure and extending into the septum. These neurons were characterized neurochemically in mice in our previous report.[1]

A moderate/intense density of KP fibers was found within the septal part of the bed nucleus of the stria terminalis (BSTMA, BSTMP, BSTLV, and BSTLP; Figures 1A, 2B–D, and 3B,C). The temporal intra-amygdala division of the BST (BSTIA; Figures 1C, 2F, and 3H) showed a selective expression of KP fibers. Other regions in the extended amygdala that also showed low/scattered expression of KP fibers were the central amygdalar nucleus (CeC and CeM; Figure 3G,H) and the medial amygdalar nucleus (MePD and MePV; Figures 2F,G and 3G,H). Sparse fibers were found in the oval nucleus of the stria terminalis (BSTLD), the basolateral amygdala (BLA), the basomedial amygdala (BMA), the lateral part of the central amygdalar nucleus (CeL), the cortico-amygdala (CoA) the nucleus of the lateral olfactory tract (NLOT), and the stria terminalis (st, Figure 1C). Compared with the

study of Brailoiu et al., here we report the presence of fibers in the anterior, medial, and cortical amygdala and the intra-amygdaloid division of the stria terminalis.

3.2.2 | Diencephalon

The *hypothalamus* contains four of the seven KP neuronal populations described in detail here and in a companion report,[1] that is, the rostral periventricular (RP3V) population mainly located in the medial preoptic area (MPO) and the anteroventral periventricular area (AVPe); the arcuate (Arc) population; the dorsomedial hypothalamus (DMH); and the ventral premammillary nucleus (PMv) (Figures 1A, 2C,D,F–H, and 3B). After a careful analysis of immunoreacted serial sections, and following the pathways of the labeled fibers, we identified some extrahypothalamic regions likely to be targets of these regions. Ascending fibers originating in the RP3V population travel lateral-dorsal-caudally toward the stria medullaris (sm) and the stria terminalis (st) conduction systems (Figure 1B). In their path, they extensively innervate the bed nucleus of the stria terminalis (Table 1). It is worth noting the presence of KP fibers innervating the border between the *medial* (*MHb*) *and lateral* (*LHb*) *habenula* (Figures 2F,G and 3B), as it is known that the main input to the habenula is the stria medullaris (*sm*). Other fibers originating in the MPO/AVPV region travel to innervate the organum vasculosum of the lamina terminalis (OVLT) and then ascend dorsally and laterally to innervate the *accumbens core* (AcbC) and the *lateral septal* regions.

We observed high-moderate densities of KP-ir fibers (see Table 1) in the caudal and ventral periventricular areas of the arcuate nucleus (Arc; Figures 1E and 2F–H). Some targets of the KP neural population in the posterior hypothalamus were identified by following the labeled axons in serially collected sections in coronal and parasagittal planes. Some fibers originating in the Arc traveled in the base of the brain, reaching the internal capsule (ic) and optic tract, through which they travel in a path to the subthalamic nucleus (STh), the lateral part of the supramammillary nucleus (SuML), and continue to the central nucleus of the amygdala (CeA). Some efferent fibers traveled caudally to innervate the ventral premammillary nucleus (VPM), the ventral tuberomammillary nucleus (VTu), and the supramammillary nucleus (SuM). Additional fibers surrounded the ventromedial hypothalamus (VMH) and traveled dorsally to innervate the anterior hypothalamic area, continuing on to innervate medial nuclei of the thalamus.

The population of weakly KP-immunopositive cells scattered in the medio-lateral dorsal hypothalamic area (DH) spanning the posterior part of the anterior hypothalamus (AHp) to the posterior hypothalamus (PH), and centered in the tuber cinereum area (TC) (Figures 1F, 2F–H, and 3B) was observed to project to adjacent zona incerta (ZI). Finally, the last population of KP neurons in the PMv was very weakly labeled, and it was not possible to identify the axonal projections.

Other regions in the hypothalamus containing KP fibers are the medial preoptic nucleus (MPO), the parastriatal nucleus (PS), the paraventricular nucleus medial magnocellular division (PVNmm) and the parvocellular division (PVNmp), and in rats also the ventral premammillary nucleus (PMv), ventral tuberomammillary nucleus (VTu), and supramammillary nucleus (SuM). A low density of KP fibers was observed in the dorsomedial hypothalamic nucleus, MPO, lateral preoptic area, periventricular hypothalamic nucleus anterior (PVa), and supraoptic nucleus (SO). Sparse fibers were found in the dorsal hypothalamus (DH), zona incerta (ZI), lateral hypothalamic area (LH), posterior hypothalamic area (PH), retrochiasmatic area (RCh), and ventromedial hypothalamic nucleus (VMH). These observations confirm and extend previous investigations of the hypothalamic KP system.[17]

In the thalamus, the highest density of fibers was observed in the paraventricular thalamic nucleus (PVT) in rats and mice (Figures 1B, 2E,F, and 3B). Low fiber densities were also observed in other nuclei of the thalamus, such as in the centromedial (CM), mediodorsal (MD), paratenial (PT), reuniens (Re), and rhomboid (Rh) nuclei. The epithalamic habenular nucleus (Hb) showed a moderate density of fibers mainly located in the border between its medial and lateral subdivisions (Figures 2F,G and 3B), with some of these fibers arriving through the stria medullaris.

3.2.3 | Mesencephalon

Within the mesencephalon, Brailoiu et al.[41] reported sparse kisspeptin-immunoreactive fibers only in the dorsomedial periaqueductal gray substance (DMPAG). In our study, this region had the highest density of kisspeptin fibers within the mesencephalon (Figures 2J and 3B). However, we also visualized scattered fibers in the central nucleus of the inferior colliculus (CIC; Figures 2I and 3D), dorsal raphe nucleus (DR; Figures 2J and 3A), and sparse fibers in the deep mesencephalic nucleus (DpMe), interpeduncular nucleus (IP), median raphe nucleus (MnR), substantia nigra (SN), intermediate and deep gray layer of the superior colliculus (DpG), supramammillary nucleus (Sum), substantia nigra pars reticulata (SNpr), and ventral tegmental area (VTA). The functional implications for those Kp projections are not yet ascertained.

3.2.4 | Metencephalon and myelencephalon

In the metencephalon and myelencephalon, we observed kisspeptin immunopositive cell bodies in the *nucleus tractus solitarius* (NTS or Sol) and *area postrema* (AP) (Figures 1G, 2L, and 3A–D). We did not observe immunopositive neurons in the caudoventrolateral or the lateral reticular nuclei (CVL and LRt), nor the spinal trigeminal tract, as reported in Brailoiu et al.[41] With respect to the density of the fibers, intense labeling was found in the lateral parabrachial nucleus (LPB; Figures 1H and 2K), the Kolliker–Fuse nucleus (KF; Figure 2K), the NTS (Figures 1G, 2L, and 3A–D), the dorsomedial part of the principal sensorial component of the trigeminal nucleus (Pr5DM; Figures 1K and 3D–G) and the locus coeruleus (LC; Figures 1I, 2K, and 3C). The rat brain also showed intense KP labeling in the gelatinous layer and the spinal nerve 5 (Figures 1J,K and 3E,F). Moderate density was observed in the superior cerebral peduncle (scp). Low intensity

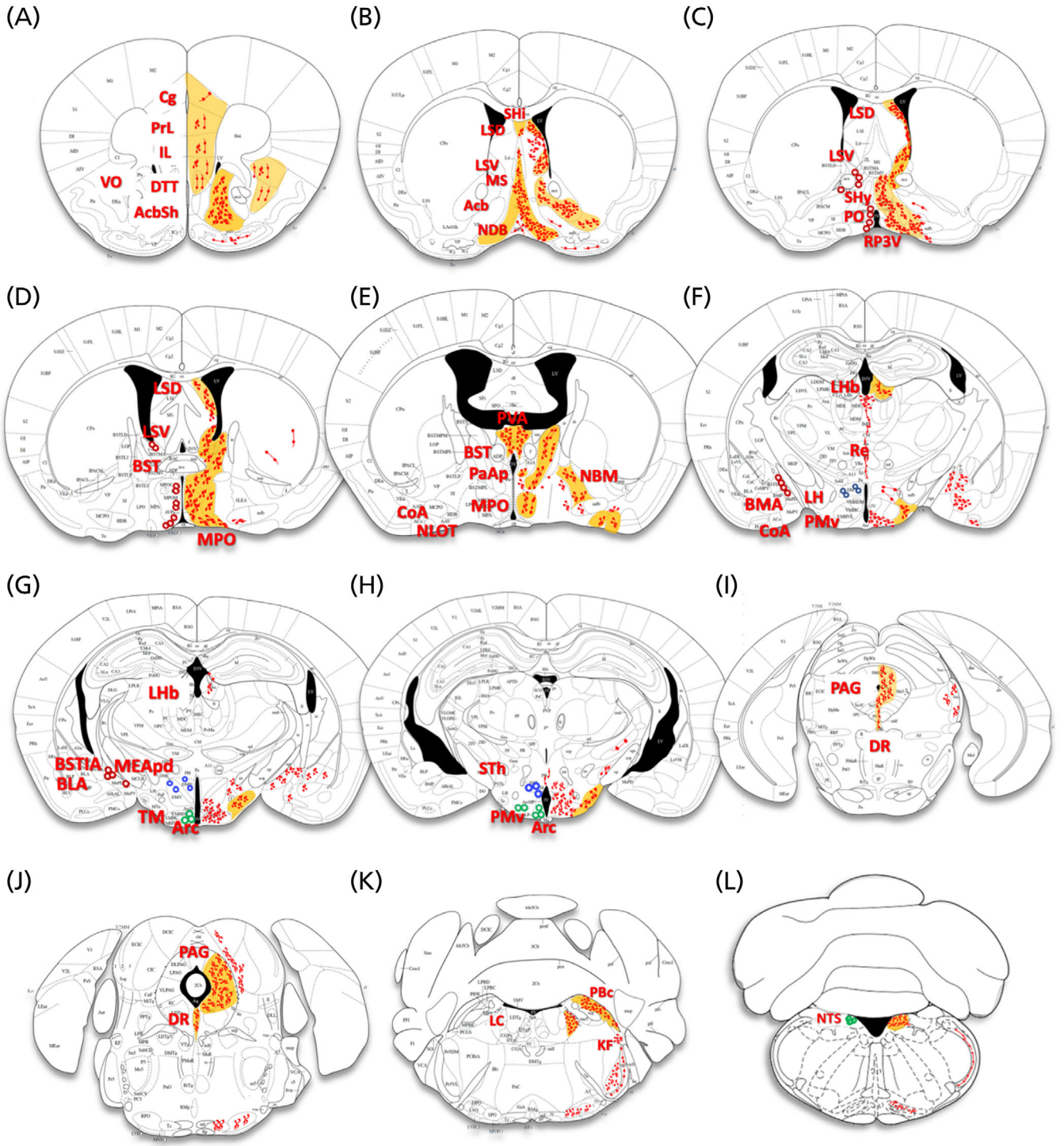

FIGURE 2 Charting to represent the distribution of kisspeptin immunoreactivity in mouse brain in register with a previous study[15] for purposes of comparison. Sequential coronal sections show KP immunoreactive cell bodies on the left, and KP immunoreactive fibers, on the right, from the seven KP cell populations. Color-filled circles symbolize the molecular signature previously reported[1]: KP-glutamatergic (green), KP-GABAergic (red), and KP with undetermined co-chemotype (blue). The distribution of KP-ir fibers are represented by red lines in the right hemisphere (the thickness of the lines has been exaggerated to ensure that the lines can be seen on the atlas planes). KP-ir fibers observed in brain areas relevant for behavioral state control are shaded in yellow: Accumbens nucleus, shell (AcbSh), septohippocampal nu. (SHi), lateral septal nu. dorsal (LSD), medial septal nu. (MS), horizontal division of nucleus of diagonal band of Broca (HDB), septohypothalamic nucleus (SHy), bed nucleus of stria terminalis (BST), medial preoptic area (MPO), paraventricular anterior parvicellular division (PaAP), nucleus basalis of Meynert (NBM), lateral habenula (LHb), lateral hypothalamus (LH), tuberomammillary nu. (TM), ventral premammillary nu. (PMv), periaqueductal grey (PAG), dorsal raphe nu. (DR), locus coeruleus (LC), lateral parabrachial nu. (LPB), and nu. of solitary tract (NTS). See Table 1 for remainder of abbreviations.

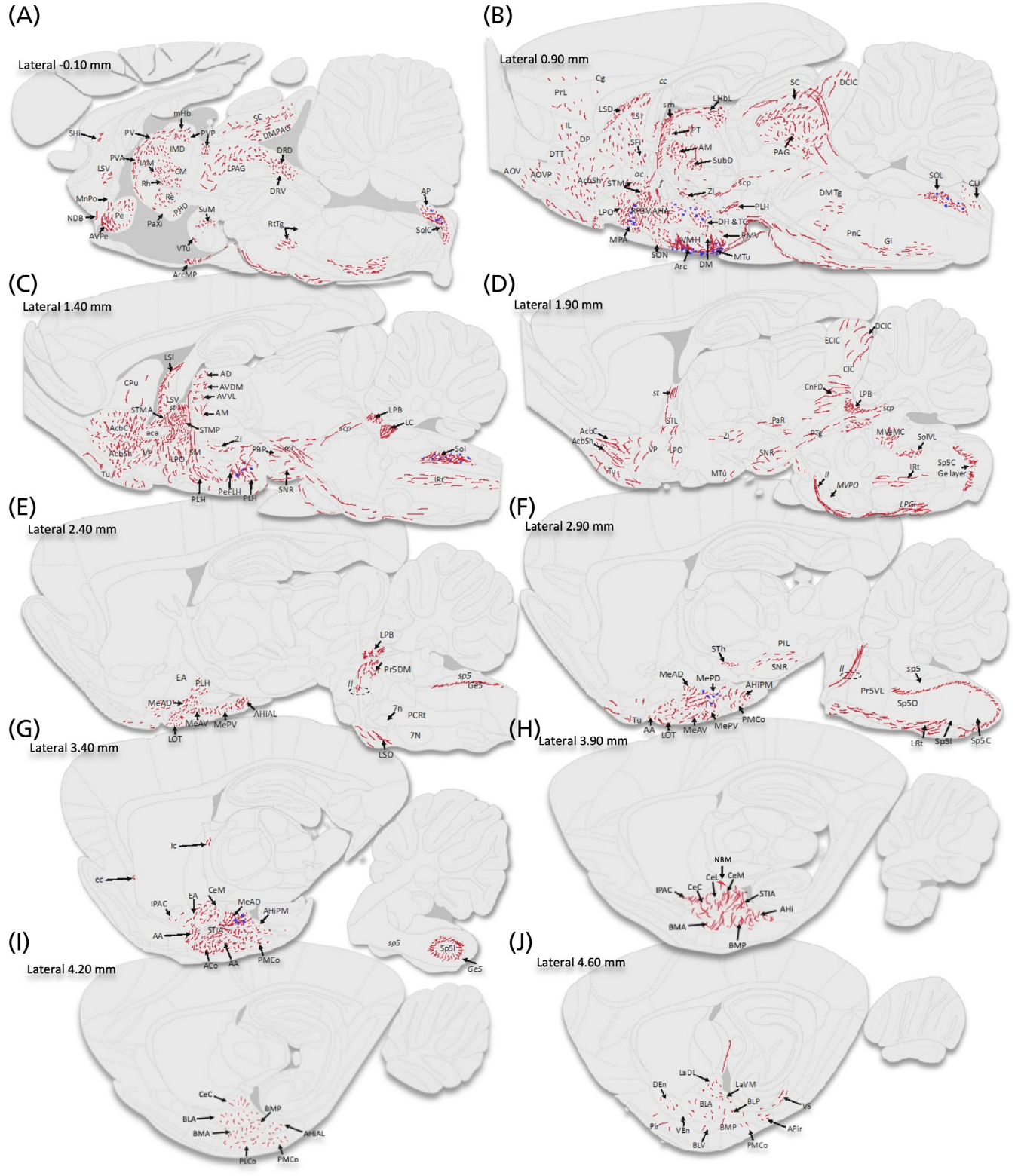

FIGURE 3 Mapping of KP immunoreactive fibers and cell bodies in rat brain in 10 septo-temporal planes based on microscopical observations. Blue dots represent KP-ir cell bodies and red lines represent KP-ir fibers. See Table 1 for abbreviations.

was observed in several nuclei of the reticular formation, including the caudoventral reticular nucleus (CVL), the gigantocellular reticular nucleus (Gi), the intermediate reticular nucleus (IRt), the lateral reticular nucleus (LRt), the medullary dorsal reticular nucleus (MdD), the parvicellular reticular nucleus (PCRt), and the rostroventrolateral reticular nucleus (RVL). Sparse fiber density was observed in the

ambiguous nucleus (Amb), lateral superior olive (LSO), ventral medullary reticular nucleus (MdV), in subregions of the pontine nucleus such as the brachium pontis (bpPn), the reticular oral part (PnO), and the reticular caudal part (PnC), and in the raphe magnus (RMg), obscurus (Rob), and pallidus (RPa).

3.3 | KP fiber density: Sex differences and short- and long-term effects of gonadectomy

Numerous studies have reported that gonadal status affects *Kiss1* expression, with KP^{Arc} expression decreased and rostral hypothalamus KP^{RP3V} expression increased by gonadal steroids.[65–67] We have also reported male and female *Kiss1* expression differences and acute sensitivity to GNX (i.e., within 4–7 weeks of GNX).[1]

We extensively studied the KP fiber distribution in male and female mice that underwent gonadectomy in young adulthood (3 month old). The experimental subjects were perfused/fixed at ages of 4–5 months (1–2 months after GNX) or 15 months (12 months after GNX). We examined KP-ir fiber densities throughout the brain, aiming to assess sex differences in KP fiber distribution and whether castration modifies the density of fibers apparent both shortly after GNX and in aged mice after early GNX, compared with intact subjects of the same age.

Figure S1 shows the cumulative (summed) fiber density charting of three young adult animals from each of four groups: male/female

TABLE 2 Semiquantitative analysis of KP immunoreactivity in regions related to sensorimotor-brain state processing in old female and male mice.

	FC	OVX	FC vs. OVX	MC	ORX	MC vs. ORX	FC vs. MC
AcbSh	+++	+++	FC ≈ OVX	++	++	MC ≈ ORX	FC > MC
Arc	+++	+++	**FC ≈ OVX**	++	++	**MC ≈ ORX**	**FC > MC**
BSTam	+++	+++	**FC ≈ OVX**	++	++	**MC ≈ ORX**	**FC > MC**
DB	+++	+++	FC ≈ OVX	+	++	MC ≈ ORX	FC > MC
DH	+	+	**FC ≈ OVX**	++	++	**MC ≈ ORX**	**FC < MC**
LC	++++	++++	FC ≈ OVX	++++	++++	MC ≈ ORX	FC ≈ MC
LSD	+	+	FC ≈ OVX	+	+	MC ≈ ORX	FC ≈ MC
MEA	+	+	**FC ≈ OVX**	+	+	**MC ≈ ORX**	**FC ≈ MC**
MS	++	++	FC ≈ OVX	+	+	MC ≈ ORX	FC > MC
NTS	++++	++++	**FC ≈ OVX**	++++	++++	**MC ≈ ORX**	**FC ≈ MC**
PaAP	+++	+++	FC ≈ OVX	++	++	MC ≈ ORX	FC > MC
PBN	++++	++++	FC ≈ OVX	++++	++++	MC ≈ ORX	FC ≈ MC
TM	+	+	FC ≈ OVX	++	++	MC ≈ ORX	FC < MC
PMv	+	+	**FC ≈ OVX**	++	++	**MC ≈ ORX**	**FC < MC**
PVA	++	++	FC ≈ OVX	+++	++++	MC < ORX	FC < MC
PVN	+++	+++	FC ≈ OVX	++	++	MC ≈ ORX	FC > MC
RP3V	+++	++++	**FC < OVX**	++	++	**MC ≈ ORX**	**FC > MC**
AH (adj SCN)	+++	+++	FC ≈ OVX	++	++	MC ≈ ORX	FC > MC
SHy	+++	++++	**FC < OVX**	++	++	**MC ≈ ORX**	**FC > MC**
STIA	+	+	FC ≈ OVX	+	+	MC ≈ ORX	FC ≈ MC
Wall 3 V	+++	+++	FC ≈ OVX	+	+	MC ≈ ORX	FC ≈ MC
ROIs adj. (f/st/sm/ac)	++	++	FC ≈ OVX	++	++	MC ≈ ORX	FC > MC

Note: Semiquantitative comparison of kisspeptin immunoreactivity in regions related to sensorial-brain state processing in old female and male mice. Scoring was based on fiber distribution using the criteria of "+" (sparse, main axons passing, without branching or axon terminals); "++," scattered, some branching; "+++," moderate, abundant branching and axon terminals; "++++," intense, extensive branching and intense axon terminals, with confluent fibers. Bold lettering regions indicate that KP immunopositive cells were also observed (e.g., Figure 4, rows of "DH," "RP3V," and "Arc"). FC: female control (intact 15 month old); OVX: 12 mo. post-ovariectomy (15 month old); MC: male control (intact 15 month old); ORX: 12 month post-orchiectomy (15 month old); AcbSh, nucleus accumbens shell; Arc, arcuate nucleus; BSTam, bed nucleus of stria terminalis, anteromedial division; DB, nucleus diagonal band de Broca; DH, dorsal hypothalamus; LC, locus coeruleus; LSD, lateral septal nucleus, dorsal division; MEA, medial amygdala; MS, medial septal nucleus; NTS, nucleus of tract solitary; PaAP, paraventricular nucleus anterior parvocellular division of the hypothalamus; PBN, parabrachial nucleus and pons; TM, tuberomammillary nucleus of the hypothalamus; PMv, premammillary nucleus, ventral subdivision of the hypothalamus; PVA, paraventricular nucleus anterior division of the thalamus; PVN, paraventricular nucleus of the hypothalamus; RP3V, rostro-periventricular complex of third ventricle of the hypothalamus; AH anterior hypothalamic area (adjacent to suprachiasmatic nucleus, SCN); SHy, septo-hypothalamic nucleus; STIA, nucleus of stria terminalis, intra-amygdalar division; Wall 3V, ependymal layer of the 3rd ventricle; ROIs adj. (f/st/sm/ac), regions of interest adjacent to brain conducting system (fornix, f, stria terminalis, st, stria medullaris, sm, anterior commissure, ac).

intact and male/female gonadectomized. The chartings were made under microscopical observation and verified by two junior and two senior experimenters of this research team. The cumulative fiber densities displayed in Figure S1 show no obvious differences among the four groups following careful analysis of KP-ir fiber density across groups. However, this may be due to compensatory and opposite regulation of KP production among multiple contributing KPergic inputs to a given region, and warrants further investigation.

We further made an analysis of tracing experiments, using KP Cre-driver mice, in ARC and RP3V, performed by the Allen Brain Institute and deposited in the Allen Brain Atlas (shown in the last two columns of the Table 1). In Figure S2, we highlight the projection targets of R3PV or Arc *Kiss1*-Cre neurons transfected with Cre-dependent AAV. The data from two *Kiss1*-Cre mice injected in the arcuate nucleus (Arc, experiments 232311236 and 232310521) and two *Kiss1*-Cre mice injected in the rostral periventricular region (R3PV, experiments 299247009 and 301989585) are reproduced in this figure. The VGAT-expressing *Kiss1* R3PV neuronal population and its projections are represented in red, and the VGLUT2-expressing *Kiss1* Arc population and its projections are represented in green. The different views show a reciprocal dense innervation between the Arc and the RP3V. Additionally, it is clear that the majority of regions in the striatum, septum, BNST, thalamus, hypothalamus, and amygdala receive convergent innervation from both Arc and RP3V Kiss1 neuronal populations.

According to our KP fiber study and analysis of the Allen Connectivity Map, a representation of the relative fiber density distribution and some identified kisspeptin pathways through the mouse brain is presented in the flat map in Figure S3. Most of the regions involved in sensorial processing, motor integration, and behavioral state control that were described and discussed previously are shown in this representation with reciprocal or convergent innervations from both KP-RP3V and KP-Arc.

Table 2 is a report of a semiquantitative analysis of brain regions concerned with brain state regulation, from four groups of 12 to 15-month-old mice, male and female intact or long-term gonadectomized. In female subjects, 19 of the 22 regions were found similar in terms of density of KP-ir fibers between old intact ("FC" stands for female control) and experimental ("OVX" stands for ovariectomy performed 12 months before perfusion/fixation) female mice. The septohypothalamic nucleus showed increased KP-ir fiber density in OVX subjects. This region, besides hosting *Kiss1/Slc32a1/Ar* expressing neurons[1] (Figure 1A,A1), receives direct $RP3V^{KP}$ and Arc^{KP} projections, as shown by the Allen Mouse Brain Atlas (Figure S2). Hence, the source of the neuronal cell group contributing to the increased KP-ir fiber density in the septohypothalamic nucleus after OVX is not clear. In the RP3V and MPO region, OVX subjects also showed an increased KP immunoreactivity (Figure 4). This region, besides hosting a KP neuronal population itself, also receives Arc^{KP} axonal projections, as demonstrated in Figure S2. In male subjects, most regions showed no apparent differences between intact ("MC" stands for male control) and orchiectomized ("ORX" stands for orchiectomy) male mice. Three regions exhibited higher densities of KP-ir fibers in the ORX group compared with the age-matched intact controls: dorsal hypothalamus (DH, Figure 4), paraventricular anterior thalamus (PVA) and tuberomammillary nucleus (TM). Also, in these three regions, the MC group showed higher densities than the FC group (Figure 4).

3.4 | Mapping of *Kiss1r* and its co-expression with *Slc32a1*, *Slc17a6*, and *Kiss1* with RNAscope methods: Assessment of *Kiss1r* distribution in the CNS and assessment of *Kiss1-Kiss1r* co-expression

3.4.1 | General description

Using RNAscope dual and multiplex ISH methods, we report here (Figure 5) the semi-quantitative expression levels of *Kiss1r*, depicted as different intensities of blue shading, in sagittal serial sections of the mouse brain. *Kiss1r* expression is diffuse and widespread (Table 3). In Figure 6, we present micrographs that correspond to the representative brain regions and subfields in Figure 5 (labeled with numbers). *Kiss1r* was observed to be strongly expressed in non-GABAergic neurons in the isocortex (for instance, the prelimbic area of the prefrontal cortex, Figure 6, panel 3; and the somatosensory cortex, panel 4; the layer 2 of the piriform cortex, panel 45), in the claustrum (panel 22) and endopiriform nucleus (panel 23), in hippocampal projection neurons (Figure 6, panel 30, dorsal hippocampus; panels 31, granule cell layer of the dentate gyrus; panels 32, 33, and 34, pyramidal layers of CA1, CA2, and CA3, respectively); the cortical amygdalar structures (Figure 6, panel 46, nucleus of the lateral olfactory tract; panel 47, cortico-amygdala; panel 49, basomedial amygdala); the mainly glutamatergic thalamic nuclei (for instance, the anteromedial nucleus of the thalamus, Figure 6, panel 29); the mainly glutamatergic hypothalamic structures (Figure 6, panel 15), such as the median preoptic nucleus (Figure 6, panel 11), the mammillary complex (Figure 6, panels 12, 15, and 19), the ventromedial hypothalamic nucleus (Figure 6, panel 16), the subthalamic nucleus (Figure 6, panel 44), the main glutamatergic midbrain structures, such as the superior colliculus (Figure 6, panel 35); the periaqueductal gray (Figure 6, panel 36); the pontine structures, such as the parabrachial complex (Figure 6, panel 37); the locus coeruleus (Figure 6, panel 38); the cerebellar granule cell layer (Figure 6, panel 44); the deep cerebellar nuclei (for instance, the interposed nucleus, Figure 6, panel 39); and the nucleus of the solitary tract (NTS) located in the dorsomedial medulla oblongata (Figure 6, panel 40). In the olfactory areas, *Kiss1r* is particularly strongly expressed, especially in VGAT-expressing neurons. In the main olfactory bulb (MOB, Figure 6, panels 1 and 2) and the accessory olfactory bulb (AOB, panels 20 and 21), *Kiss1r* is strongly expressed in the periglomerular and granule GABAergic neurons. Other prominent GABAergic structures with strong *Kiss1r* expression are the medial (Figure 6, panel 6) and lateral (panel 5) septal nuclei, the nucleus accumbens (panel 7), the olfactory tubercle (panel 9), the striatal caudate putamen (panel 24), the pallidal bed nucleus of the stria terminalis (panel 28), the diagonal band of Broca (panel 26), the reticular thalamic nucleus (panel 29), the hypothalamic lateral preoptic area (panel 27), the suprachiasmatic nucleus (panel 10), the tuberomammillary nucleus (panel 12), the supramammillary nucleus (panel 19), and the central amygdala (panel 50).

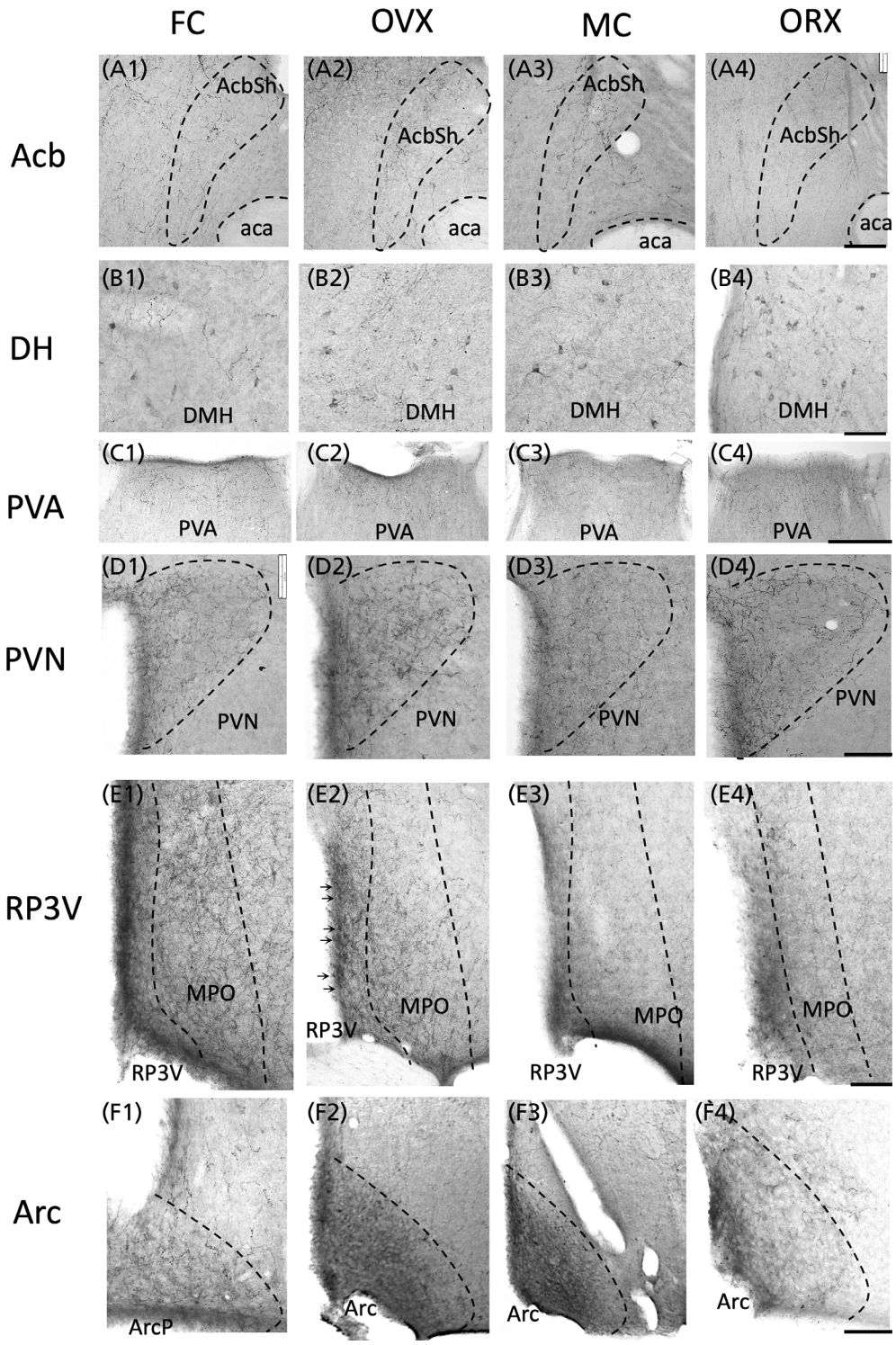

FIGURE 4 Examples of KP-ir fiber density in old mice: Comparison of four groups. FC: Samples from female control, intact mice of 15-month-old; OVX: Female mice undergoing ovariectomy in young adulthood (3-month-old) and perfused/fixed (12 months after OVX); MC: Male intact mice; ORX: Male mice undergoing orchiectomy in young adulthood (3 month old) and perfused/fixed (12 months after ORX). Acb, nucleus accumbens; AcbSh, nucleus accumbens shell: Arc, arcuate hypothalamic n.; ArcP, arcuate hypothalamic n. posterior; DH, dorsal hypothalamus; DMH, dorsomedial hypothalamus; PVA, paraventricular nucleus anterior division of the thalamus; PVN, paraventricular nucleus of the hypothalamus; RP3V, rostro-periventricular complex of third ventricle of the hypothalamus. Scale bars: 100 μm.

3.4.2 | *Kiss1r* expressed in *Kiss1* neurons in the hypothalamus

Kiss1r was also observed to be co-expressed with some *Kiss1*-expressing neurons in hypothalamic RP3V and Arc regions in sagittal sections using the 4-channel RNAscope LS Multiplex Fluorescent Assay against mRNA for kisspeptin receptor (*Kiss1r*) and kisspeptin (*Kiss1*), suggesting potential autocrine and paracrine components of KP signaling in the hypothalamus.

In Figure 6, panel 14, we show a confocal microphotograph obtained using the Stellaris confocal microscope (Leica Microsystems) on a parasagittal section of the RP3V of a female mouse. *Kiss1r* labeling (red dots) was clearly seen to co-localize with *Kiss1* (green dots) expressed in cells (6 co-localized cases among a total of 6 *Kiss1*-expressing neurons), which also co-expressed both *Slc32a1* (mRNA encoding the vesicular GABA transporter, VGAT) and *Slc17a6* (mRNA encoding the vesicular glutamate transporter 2, VGluT2) (Figure 6, panel 14, quadruple arrows). The four insets on the right

TABLE 3 Distribution, cell types, and strength* of main *Kiss1r* expressing cell groups in the mouse brain with comparison of co-expression of *Slc32a1* (VGAT).

Cell group / sub-field**	Co-expressing with Slc32a1	No Slc32a1 co-expressing
Cerebrum: cortical plate		
Olfactory area		
Main olfactory bulb (MOB) * **		
granular cell layer (gr)	+++	+
inner plexiform layer (ipl)	-	-
mitral cell layer (mi)	+	+++
outer plexiform layer (opl)	-	+
glomerular layer (gl)	+++	+
Accessory olfactory bulb (AOB) * **	n/r	+
mitral cell layer (mi)	+	+++
glomerular layer (gl)	++++	+
granular layer (gr)	++++	+
Anterior olfactory n. (AON)	+	++
Taenia tecta (TT)	+	++
Piriform area: Pir2	-	+++
Piriform area: Pir3	-	++
N. lat. olfactory tract (NLOT)	-	+++
Cortical amygdalar area (CoA)	-	+++
Hippocampal formation * **		
Dentate gyrus granule cell layer	+	++++
CA1, pyramidal cell layer	+	++++
CA2, pyramidal cell layer	+	++++
CA3, pyramidal cell layer	+	++++
hilus	++	++
subiculum	++	++
Isocortex * **		
Layer V	+	++
Layer VI	+	+++
Agranular insular cortex * **	+	++++
Somatomotor areas * **	+	+++
Agranular insular cortex * **	+	+++
Orbital frontal cortex (OFC)		
OFC 1	+	++
OFC 2/3	+	+++
OFC 5	+	+++
Prefrontal Cortex		
Ant cingulate cortex (ACC)		
ACC 2/3:	+	+++
ACC 5:	++	+++
Prelimbic (PL)		
PL 2/3	+	+++
PL 5	++	+++
Infralimbic (IL)		
IL 2/3	++	+++
IL 5	++	+++
Prim somatosensory a. SSp, * **		
SSp 1	+	++
SSp 2/3	+	++
SSp 4 (mouth)	+	++
SSp 5	+	++
SSp 6a	+	+++
Gustatory areas (GU) * **	+	++
Auditory area * **	+	++
Visual area * **	+	++
Visceral area (VISC) * **	+	++
Temporal association area* **	+	+++
Ectorhinal area * **	+	+++
Perirhinal area * **	+	++
Retrosplenial area * **	+	+++
Post parietal association area * **	+	+++
Cortical subplate		
Claustrum * **	+	++
Endopiriform nucleus	+	++
Lateral amygdalar nucleus (LA)	+	+++
Post amygdalar nucleus (PA)	+	+++
Basomedial amygdala (BMA)	+	+++
Basolateral amygdala (BLA)	+	+++
Cerebral nuclei		
Striatum		
Caudate putamen	+++	+
Lateral septal nucleus (LS)	++	++
Septo-hypothalamic nucleus (SHy)	+++	+++
Midbrain raphe nuclei	+	+++
Pedunculopontine n.	+	++
Dorsal n. raphe	++	++
Pons		
N. lateral lemniscus	+	+
Principal sensorial nucleus of trigeminal nerve	-	++
Koelliker-Fuse subnucleus	-	++
Parabrachial n. lateral div.	-	+++
Superior olivary comp (lat)	-	++
Tegmental reticular n.	++	+++
Dorsal tegmental n.	++	+++
Pontine gray	-	++++
Pontine central gray	++	+++
Supratrigeminal nucleus	++	++
Locus Coeruleus (state related)	-	++++
Laterodorsal tegmental n.	++	+++
Pontine reticular n.	++	+++
Superior central n. raphe	++	++
Medulla		
N. tractus solitarii medial	+	+++
N. tractus solitarii lateral	+	+++
Hypoglossal (XII) n.	+	++
Dorsal motor n. of the Vagus nerve (X)	+	+++

Cell group / sub-field**	Co-expressing with Slc32a1	No Slc32a1 co-expressing
Anterior amygdala area (AAA)	++	+
Central amygdalar nucleus (CEA)	++	+
Medial amygdalar nucleus (MEA)	++	+
Pallidum (basal forebrain)		
Medial Septal nucleus (MS)	++	++
Bed nucleus of stria terminalis (BNST)	++	++
Nucleus basalis of Meynert	+	+++
Globus pallidus	+	++
Substantia innominata (SI)	+	++
Nucleus of diagonal band of Broca (NDB)	+	++
Nucleus Accumbens	++	+
Brain stem, inter-brain		
Thalamus		
Somato-motor related		
Subparafacicular nucleus, magnocellular part	-	+++
Subparafacicular area	-	+++
Peripeduncular nucleus	-	+++
Medial geniculate complex	-	+++
Polymodal association cortex related		
Lat. posterior n. thal	-	+++
Post. limiting nucleus	-	+++
Suprageniculate n.	-	+++
Anterodorsal n.	-	+++
Anteromedial n.	-	++
Parataenial n.	-	++
Intermedial n.	-	+++
Laterodorsal n.	-	+++
Centrolateral n	-	+++
Intermediodorsal n.	-	+++
Mediodorsal n.	-	+++
Pariventricular n.	-	+++
Parateanial n.	-	+++
N. of reuniens[n2]	-	+++
Posterior pretectal n.	-	+++
Precommissural n.	-	+++
Reticular nucleus of the thalamus (Rt)	+++	-
Epithalamus		
Medial habenula	-	++++
Lateral habenula	+	++++
Hypothalamus		
Paraventricular n. (PVN)	+	++
Arcuate Nucleus	+++	-
Suprachiasmatic nucleus	+++	+
Rostro-periventricular of the 3V (RP3V)	+++	++
Anterodorsal preoptic n.	++	++
Anteroventral n.	+++	++
Dorsomedial n.	+++	++
Median preoptic n.	++	++
Medial preoptic area	++	++
Vascular organ of lamina terminalis	-	-
Lateral preoptic area (LPO)	++	+
Anterior hyp. area (AH)	+++	+
Premammilary n. (PM)	-	+++++
Lateral mammillary n.	-	+++++
Medial mammillary n. (MM)	-	+++++
Supramammillary n.(SUM)	++	++
Median preoptic n. (MnPO)	+	+++
Lateral hyp. area (LH)	++	++
Subthalamic nucleus (STN)	-	+++++
Retrochiasmatic area	+++	++
Tuberomammilary nucleus (TM, magnocellular subnucleus MTu)	+++	+++
Zona incerta (ZI)	++	+
Ventromedial hyp. n (VMH)	-	+++++
Post. hypothalamic n.	+	+
Midbrain		
Superior colliculus, sensorial (SCS)	+	+++
Superior colliculus, motor (SCM)	+	++
Inf. Colliculus (IC)	++	++
N. of the brachium of IC (BIC)	+	+
Ventral tegmental area (VTA)	+	+++
Sustantia nigra reticulata	+	+++
Midbrain reticular n.	+	++
Periaqueductal gray	++	+++
Dorsal cochlear n.	-	++
Ventral cochlear n.	-	++
Spinal n. trigeminal	+	++
N. prepositus	-	+++
Facial motor n. (VII)	++	++
N. ambiguus	++	+++
Magnocellular reticular n.	++	+++
Spinal vestibular n.	+++	++
N. X	+	++
N. raphe magnus (state related)	+	+++
N. raphe pallidus (state related)	+	+++
N. raphe obscurus (state rel.)	+	+++
Cuneate n.	+	+
Inferior olivary	+	+++
Cerebellar cortex		
Purkinje's cells	-	-
Golgi's cells	+	-
Granule cell layer ***	-	++++
Cerebellar nuclei		
Interposed n. ***	+	+
Dentate n. ***	-	++
Fastigial n. ***	+	++

*Semiquantitative annotations are used here (the percentage of expressing cell/total Nissl stained nuclei); "−," not detectable; "+," <20%; "++," >20% and <40%; "+++," >40% and <60%; "++++," >60% and <80%; "+++++," >80%.**Functional neuroanatomy order and annotations are based on the Allen Institute Mouse Reference Atlas.

***"Mismatched" regions: regions with a remarkable presence of Kiss1r, however, apparently lacking KP-ir fibers.

side display the single-channel micrographs for each mRNA probe of the cell indicated with a thin red arrow (in the center of the main micrograph). Note that the thin arrow in each channel is automatically generated and inserted by Leica Application Suite (LAS) software to indicate the same *X*–*Y* coordinates. Numerous VGluT2-expressing cells in the adjacent location, lacking mRNAs for KP or VGAT, also co-

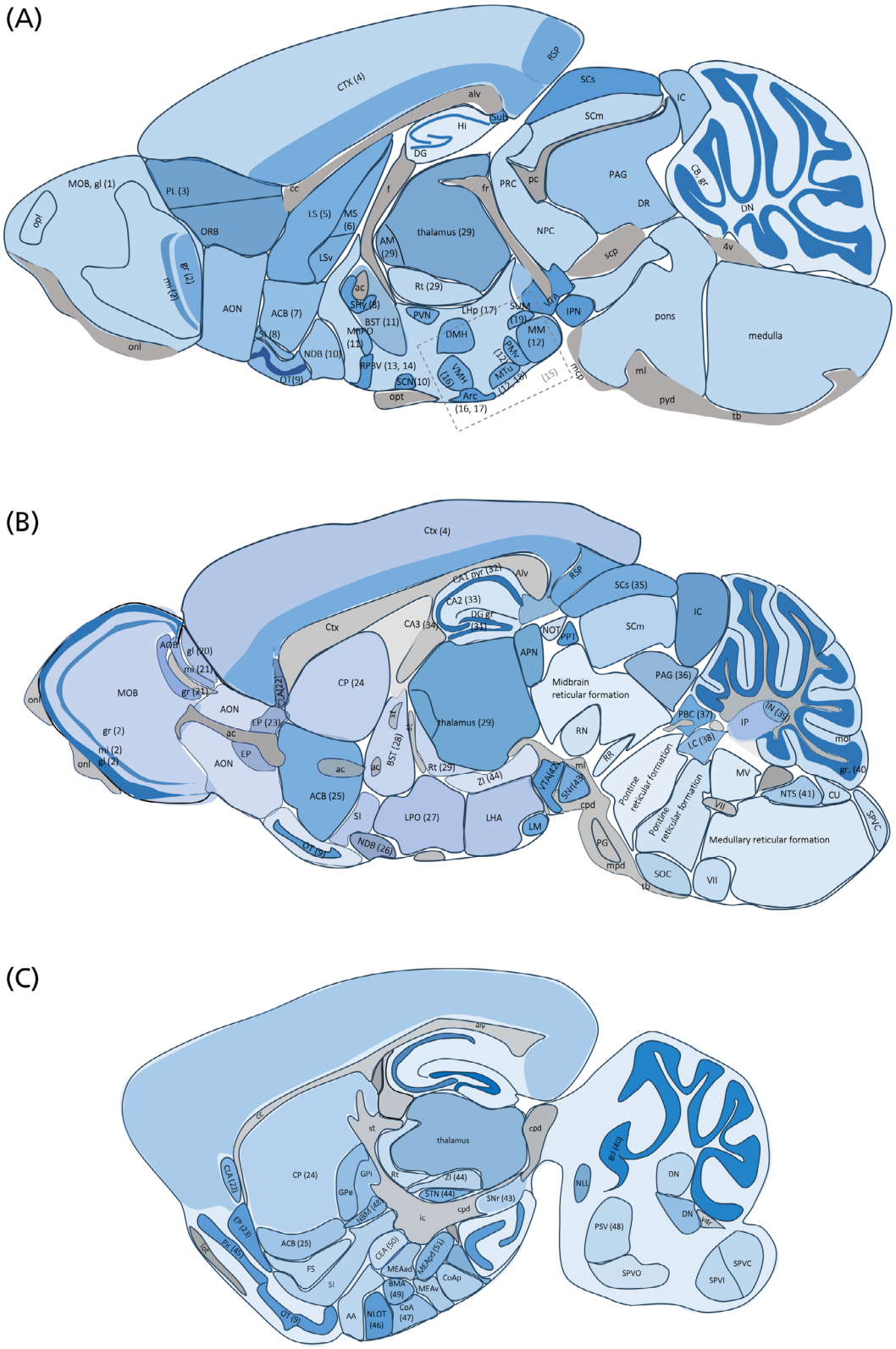

FIGURE 5 Legend on next page.

expressed Kiss1r (indicated with bicolor arrows). Figure 6, panel 17, depicts a field within the Arc nucleus, displaying three Kiss1-expressing neurons (green dots, indicated with green arrows). The insets displayed on the right side are separate channels with thin red arrows generated by the computing software, indicating the same *X*–*Y* coordinates of the cell in the center of the main panel. Only one of the three *Kiss1*-expressing cells co-expressed *Kiss1r*, as well as Slc17a6 (triple arrows).

Panel 12 of Figure 6 depicts the expression of *Kiss1r* in each of the cells in the ventral division of the premammillary nucleus (PMv), a region recently reported to host the newly discovered KP population. Most neurons neighboring *Kiss1*-expressing cells also expressed *Kiss1r*.

It is worth noting that the multiplex-ISH observations were obtained from sagittal samples from one male and one female mouse, providing a preliminary basis for more extensive quantitative studies of *Kiss1/Kiss1r* co-expression under various conditions. Such further studies should be useful to determine functional significance for diverse kisspeptin autocrine, paracrine, and perhaps synaptocrine[68,69] regulation, given that previous studies[33,70] have not reported co-expression in *Kiss1* and *Kiss1r* hypothalamic neurons.

3.4.3 | A mismatch between strong expression regions of *Kiss1r* and the KP-ir fiber distribution

A mismatch in terms of brain regional distributions between the mRNA for the KP receptor of mouse, *Kiss1r*, and the KP immunoreactive fibers (KP-ir) is highlighted in Table 3: regions with prominent *Kiss1r* expression but without observed KP-ir fibers are indicated with "***." These regions include the main olfactory bulb (MOB), the accessory olfactory bulb (AOB), and the hippocampal formation, with the strongest expression seen in the granule cell layer (gcl) of the dorsal dentate gyrus, the pyramidal cell layer (pcl) of the CA1, CA2, and CA3, as well as in the hilus and the subiculum. The isocortex, which includes the insular cortex, primary somatosensory cortex, gustatory, auditory, visual, visceral, temporal association, entorhinal, perirhinal, retrosplenial, post-parietal association areas, and claustrum, also exhibited high expression of *Kiss1r* that is not matched by notable KP immunoreactive fibers.

Three hypothetical explanations for this mismatch are discussed in Section 4.4.

4 | GENERAL DISCUSSION AND CONCLUSIONS

This report continues our recent work[1] in which we provided a chemotype of seven *Kiss1*-expressing neuronal populations in the mouse brain. Our current study focuses on the distribution and density of kisspeptin (KP)-immunoreactive (KP-ir) fibers and cell bodies throughout the brains of mice and rats, as well as the distribution of the *Kiss1* receptor (*Kiss1r*) in register with GABAergic neurons throughout the mouse brain and kisspeptinergic neurons in the hypothalamus.

4.1 | Prominent KP fiber distribution in sensorial and brain state control centers: Aging and sex steroids

Our anatomical observations regarding the regional distribution of KP-ir fibers and cells in young and aged mice, along with the effects of short- and long-term gonadectomy, underscore the broader roles of KP signaling beyond reproductive functions, potentially including its involvement in sensory processing, behavioral state control, and emotional regulation. Additionally, the lack of a significant age-related decline in KP immunoreactivity—contrary to what is observed in other neuropeptide systems—raises intriguing questions about its role in aging-related diseases such as cancer,[71] and neurodegeneration,[72] as well as the mechanisms underlying its stability.[42]

Aging has been associated with reductions in the density or functionality of various neuropeptide systems, such as neuropeptide Y (NPY), pituitary adenylate cyclase-activating polypeptide (PACAP), and pro-opiomelanocortin (POMC),[73–75] which often correlate with cognitive decline, disrupted behavioral states, and changes in physiological homeostasis. With regard to the kisspeptin (KP) system, contrasting effects of aging on KP expression have been documented. It has been reported through immunohistochemistry (IHC) that in aged

FIGURE 5 Mapping of Kiss1r (RNA encoding KP receptor) expression (symbolized by the intensity of blue shading) in three septo-temporal planes (A–C) based on microscopical observation reported in Table 3. Numbers following region-abbreviations correspond to the panel numbers of Figure 6. ACB, nucleus accumbens; AM, anteromedial nucleus of thalamus; AOB gr, granule cell layer AOB; AOB ipl, inner plexiform layer AOB; AOB mi, mitral cell layer of the AOB; AOB opl, outer plexiform layer of the AOB; AOB gl, glomerular layer of the AOB; MOB, main olfactory bulb; Arc, arcuate hypothalamic n.; BMA, basomedial amygdala; BST, bed nucleus of stria terminalis; CEA, central amygdala; CLA, claustrum; CoA, corticoamygdala; CP, caudoputamen; DC, dentate gyrus; EP, endopiriform n.; gcl, granule cell layer of DG; gr, cerebellar granule cell layer; LC, locus coeruleus; LPO, lateral preoptic area; LS, lateral septal nu.; MEA, medial amygdala; MnPO, median preoptic n.; MOB, main olfactory bulb; MOB gl, glomerular layer of the MOB; MOB gr, granule cell layer MOB; MOB ipl, inner plexiform layer MOB; MOB mi, mitral cell layer MOB; MOB opl, outer plexiform layer MOB; Mol, cerebellar molecular cell layer; MS, medial septal nu.; NBM, nucleus basalis of Meynert; NDB, diagonal band nucleus; NLOT, nucleus of lateral olfactory tract; NTS, nucleus tractus solitarii; OT, olfactory tubercle; PAG, periaqueductal grey; PB, parabrachial nu.; PC, Purkinje cell; PfC, prefrontal cortex; Pir, piriform cortex; PL, prelimbic area; plc, pyramidal cell layer; PMv, premammillary n., ventral; RP3V, rostro-periventricular nu. of 3rd ventricle; Rt, reticular thalamic nucleus; SC, superior colliculus; SCN, suprachiasmatic nu.; scp, superior cerebellar peduncle; SHy, septo-hypothalamic nu.; SNr, substantia nigra reticulata; SS, somatosensorial cortex; STN, subthalamic nucleus; SUM, supramammillary nu.; VTM, tuberomammillary nu., ventral; VMN, ventromedial hypothalamic nu.; VTA, ventral tegmental area; ZI, zona incerta.

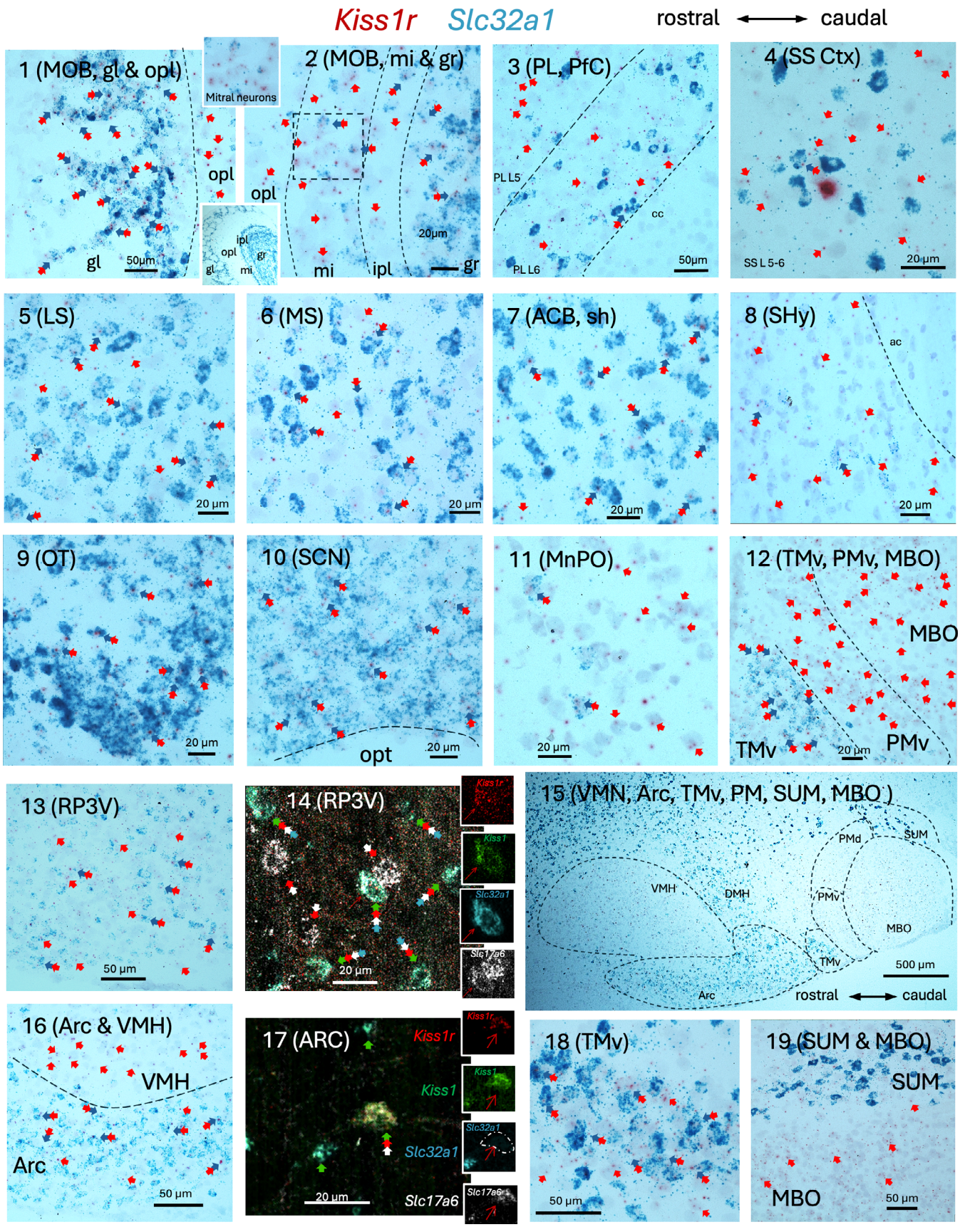

Figure 6 Legend on next page.

male and female rats, KNDy-ARC neurons reduce their expression of KP, dynorphin, and neurokinin B peptides.[76] In contrast, studies in monkeys and postmortem human tissue reveal that aging correlates with a significant increase in the size of KiSS-1 mRNA-expressing neurons, as well as an increase in the number of labeled cells and autoradiographic grains per neuron.[77]

The distribution patterns we report here indicate that many hypothalamic and extrahypothalamic regions are innervated by kisspeptin as strongly as the classical hypothalamic regions known for regulating the hypothalamic–pituitary–gonadal (HPG) axis. These may serve both reproduction-related behavioral functions, as well as non-reproductive functions. Indeed, many of these regions are critical for

FIGURE 6 Examples illustrating Kiss1r co-expression with GABAergic neurons (Slc32a1 mRNA encoding VGAT) in cortical and subcortical regions from sagittal sections. Co-expression Kiss1r with Kiss1 (mRNA encoding kisspeptin), Slc17a6 (mRNA encoding VGluT2) and Sla32a1, was examined at the RP3V and Arc regions (panels 14, 17, and 39). Panels 1 and 2: MOB, main olfactory bulb; gl, glomerular layer; opl, outer plexiform layer; mi, mitral cell layer; ipl, inner plexiform layer; gr, granule cell layer. N.B. Kiss1r (red dots) is widely expressed in the MOB periglomerular cells which are inhibitory interneurons (Slc32a1, blue patches, co-expressing, bicolor arrows in panel 1). Kiss1r is also widely expressed in the opl, not Slc32a1 expressing cells (red arrows) (panel 1). The principal projection cells in MOB, the mitral cells, mi, are strongly expressing the Kiss1r (panel 2), as well as the GABAergic neurons in the granule cell layer (gr). Panel 3: PL, prelimbic area of prefrontal cortex (PfC), most Kiss1r labeling (red arrows) are not on Slc32a1 expressing neurons. Panel 4: Somatosensorial cortex (SS Ctx), layer 5–6, most Kiss1r labeling (red arrows) are not on Slc32a1 expressing neurons. In lateral, medial septal nuclei (LS, panel 5, and MS, panel 6) and nucleus accumbens (ACB, panel 7), the Kiss1r was mainly found in Slc32a1 expressing (GABAergic) neurons (bicolor double arrows). Panel 8: Shy, septo-hypothalamic nucleus, the Kiss1r labeling are main in none-Scl32a1 cells (red arrows). Panel 9 and 10: OT, olfactory tubercle and SCN, suprachiasmatic nucleus, the Kiss1r is almost exclusively expressed in the Scl32a1 expressing neurons (bicolor double arrows). Panel 11: MnPO, median preoptic nucleus, Kiss1r is expressed in both GABAergic and no-GABAergic cells. In panel 12, three adjacent hypothalamic regions are displayed. TMv: Tuberomammillary nucleus ventral division, most GABAergic neurons expressed Kiss1; PMv, premammillary nucleus, ventral division, and MBO, mammillary body, almost all the cells expressed Kiss1r on Slc32a1-negative cells. N.B. the wide and strong expression of Kiss1r in PMv that almost every Nissl-stained nucleus contained Kiss1r strongly suggest that those kisspeptin expressing neurons demonstrated in a recent report[1] use autocrine signaling mechanism. Panel 13: RP3V, rostro-periventricular n. of 3rd ventricle, where Kiss1r is widely expressed in both Slc32a1 positive and negative cells. Panel 14: Examination of RP3V using 4 channels RNAscope LS Multiplex Fluorescent Assay method against mRNA for kisspeptin receptor (Kiss1r, red dots), kisspeptin (Kiss1, green dots), VGAT (Slc32a1, blue dots) and VGLUT2 (Slc17a6, white dots). Six out nine cells (6/9) in this confocal microphotograph were found co-expressing the 4 mRNAs, indicated with quadri-color-arrows. Insets show 4-channel separated screenshots of the cell in the center. The red thin arrows, generated by the Leica Application Suite (LAS) software, indicate the very same coordinates in each channel and the overlay. The three cells which were not Kiss1+ (not Slc32a1+) were all Slc17a6 (VGLUT2) expressing as well as Kiss1r expressing. Panel 15: Low magnification micrograph showing relevant hypothalamic nuclei regarding Kiss1r and Slc32a1 expression. VMN, ventromedial hypothalamic n., Arc, arcuate hypothalamic n., TMv, tuberomammillary n. ventral division, PM, premammillary n. ventral and dorsal divisions, SUM, supramammillary n., MBO, mammillary body. Panel 16: Kiss1r in ventromedial hypothalamic n. (VMH) is widely and exclusively expressed in no-Slc32a1 cells. In contrast, in the arcuate hypothalamic n. (Arc), the Kiss1r is expressed in both Slc32a1 expressing cells (bicolor arrows) and cells which do not express Slc32a1. Panel 17: Examination of Arc using 4 channels RNAscope LS Multiplex Fluorescent Assay against mRNA for kisspeptin receptor (Kiss1r, red dots), kisspeptin (Kiss1, green dots), VGAT (Slc32a1, blue dots) and VGLUT2 (Slc17a6 white dots). One out of three (1/3) cells in this confocal microphotograph was found co-expressing the mRNAs for Kiss1r, and Slc17a6 Kiss1 expressing but not the Slc32a1 (indicated with tricolor arrows). Insets show 4-channel separated screenshots of the cell in the center. The red thin arrows, generated by the Leica Application Suite (LAS) software, indicate the very same coordinates in each channel. Panel 18: TMv, tuberomammillary n. ventral division: Kiss1r is expressed in both Slc23a1, and no-Slc32a1 cells. Panel 19: Kiss1r is strongly expressed in MBO as already shown in panel 12 but weakly expressed in the supramammillary n. (SUM). Panels 20 and 21: Kiss1r expression in accessory olfactory bulb (AOB) with similar patterns of MOB (see panels 1 and 2), that is, strongly co-expressed with Slc32a1 (VGAT expressing cells) in periglomerular cells in gl. and granule cells. In the projection layer (mi), the mitral cells which do not express Slc32a, also strongly expressed Kiss1r. The AOB is primarily involved in processing pheromonal signals detected by the vomeronasal organ (VNO) and is critical for mediating social and reproductive behaviors. Panel 22 and 23: Claustrum (CLA) and endopiriform n. (EP), Kiss1r is mainly expressed in no-Slc32a1 neurons. Kiss1r is mainly co-expressed in Slc32a1 (VGAT expressing) neurons in caudoputamen (CP, panel 24), nucleus accumbens (ACB, panel 25), nucleus of diagonal band (NDB, panel 26), bed nucleus of stria terminalis (BST, panel 28) and reticular thalamic nucleus (Rt, panel 29, left). Panel 27 shows the mixed expression of Kiss1r, in both Slc32a1-positive and -negative cells in the lateral preoptic area (LPO). In thalamus, the Kiss1r is widely expressed (panel 29, right half). In the hippocampal formation, Kiss1r is strongly expressed in the projection neurons (Panels 30–34). Panel 35 and 36: Midbrain superior colliculus (SC) and periaqueductal grey (PAG), Kiss1r mainly expressed in no-Slc32a1 expressing cells. Panel 37 and 38: Pontine parabrachial n. (PB) and locus coeruleus (LC), Kiss1r mainly expressed in no-Slc32a1 expressing cells. Panel 39: Examination of cerebellum using 4 channels RNAscope LS Multiplex Fluorescent Assay against mRNA for kisspeptin (negative and not showing), kisspeptin receptor (Kiss1r, red dots), VGAT (Slc32a1, light blue patches) and VGLUT2 (Slc17a6, white patches). Interposed nucleus was found co-expressing the mRNAs for Kiss1r and Slc17a6 but not the Slc32a1. The multicolor arrows, generated by the Leica Application Suite (LAS) software, indicate the very same coordinates in each channel. Panel 40: Wide expression of Kiss1r in cerebellar granule cell layer (gr). Panel 41: Wide expression of Kiss1r in the brainstem nucleus tractus solitarii (NTS). Panels 42–44, midbrain ventral tegmental area (VTA), substantia nigra reticulata (SNr), interbrain subthalamic nucleus (STN) and zona incerta (ZI). In the regions 40–44, the Kiss1r is expressed almost exclusively in Slc32a1-negative cells. Panel 45 shows the strong Kiss1r expression in pyramidal cell layer of the piriform cortex (Pir). Panel 46, 47, 49, and 51: Nucleus of lateral olfactory tract (NLOT), cortico-amygdalar nucleus (CoA), basomedial amygdala (BMA), and medial amygdala (MeA): Kiss1r is widely expressed in Slc32a1-negative cells of these basal forebrain structures. Panel 48: Nucleus basalis of Meynert (NBM), a group of cholinergic neurons located in the basal forebrain, widely expressed the Kiss1r. Panel 50: CEA, central amygdala, Kiss1r is mainly expressed in Slc32a1-positive cells. Scale bars: Indicated for each micrograph.

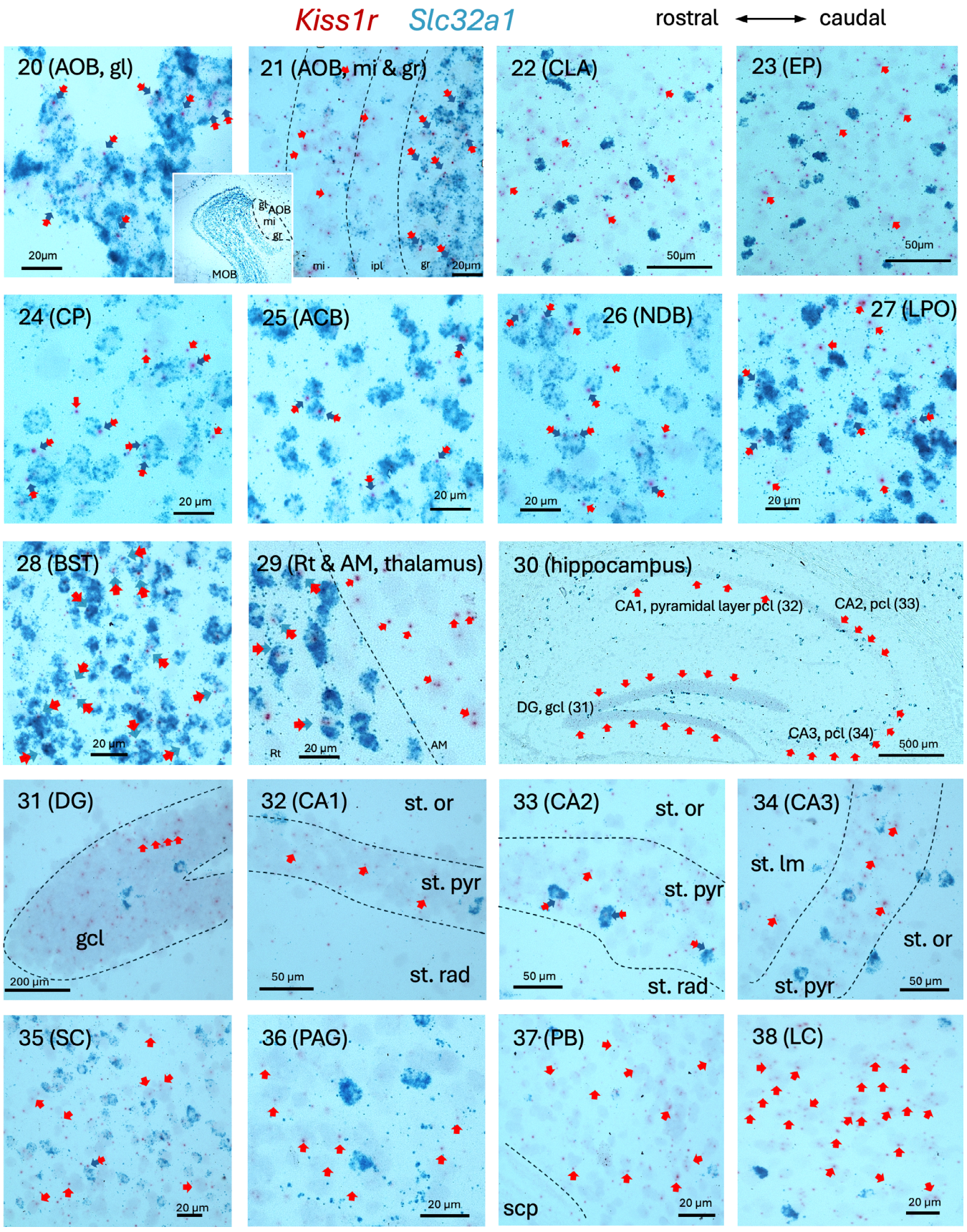

FIGURE 6 (Continued)

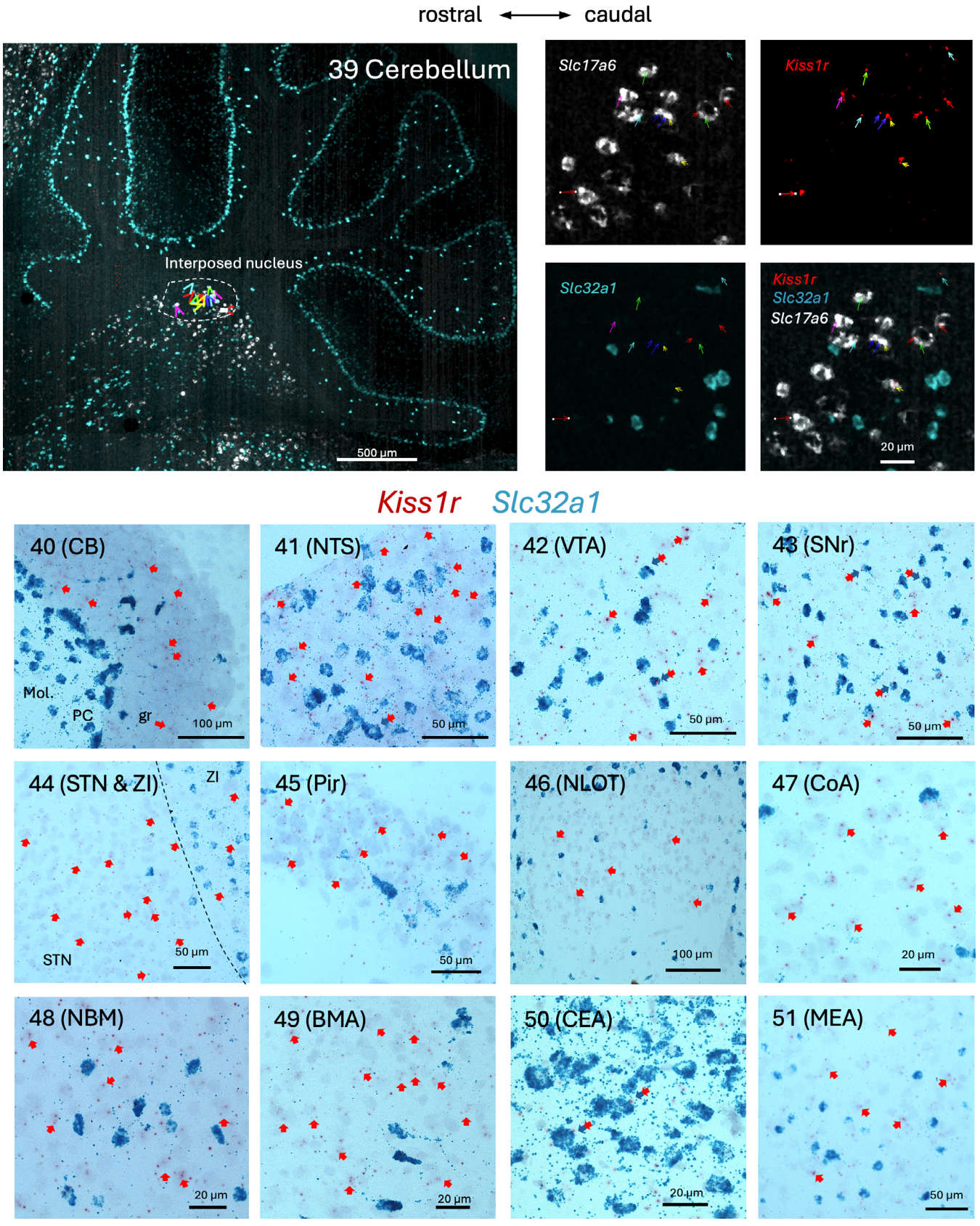

FIGURE 6 (Continued)

regulating brain states, including telencephalic cortical areas basal forebrain (diagonal band nucleus, accumbens nucleus, septohypothalamic nucleus, medial and lateral septal nuclei), diencephalic structures (thalamic regions which are crucial for cortical activation, arousal, and control of awareness such as reuniens nucleus, paraventricular thalamic nucleus anterior),[78] hypothalamic median preoptic nucleus, suprachiasmatic nucleus, complex of the bed nucleus of stria terminalis, and nucleus basalis of Meynert, midbrain regions (periaqueductal grey, dorsal raphe nucleus, substantia nigra, and ventral tegmental area), and metencephalic areas such as the raphe nuclei, reticular formation, and locus coeruleus (see Section 3.2 for more focused discussion).

A highlight of this study is the analysis of brains from aged male and female mice gonadectomized early in the lifespan. Notably, the KP fiber density in regions associated with reproductive and non-reproductive functions was found to be similar to, or even increased in, gonadectomized animals compared with controls, suggesting that the KP system remains functional even after reproductive senescence.

KP signaling modulates sexual and emotional processing in humans.[14] Ogawa et al. found that kisspeptin in the habenula of zebrafish plays a role in fear responses,[12,79] suggesting that it may facilitate the removal of fear, which is essential for maintaining reproductive capabilities under stress. Kisspeptin's influence on anxiety-related behaviors has also been documented in kisspeptin receptor-deleted male mice, indicating that kisspeptin signaling may play a role in facilitating the activity of anxiogenic neural circuits operative in the elevated plus maze test (EPM).[8]

The interaction between kisspeptin and other neuropeptides was suggested by the work of Stincic et al., in which inputs to the PVN and DMH from presumptive ARC^{KP} and $R3PV^{KP}$ neurons were demonstrated by electrophysiology and optogenetics experiments, suggesting the interaction of the KP system with other neuropeptide systems involved in homeostatic and autonomic regulation.[80] Effects of ICV injection of KP-13 suggest that this peptide stimulates the HPA axis, induces hyperthermia, activates motor behavior, and causes anxiety in rats.[81]

We have reported in this study that a high density of KP fibers is present in areas related to pain sensory processing, such as the principal sensory trigeminal nucleus, the gelatinous layer of the trigeminal nucleus, and the periaqueductal gray. In the literature, only a few studies have investigated KP's role in the modulation of the perception of exteroceptive or interoceptive non-reproductive stimuli. It has been shown that KP-10 activates calcium signaling pathways in cultured dorsal root ganglion cells, suggesting a possible participation in pain modulation.[82] Other regions classically involved in sensory processing have moderate/dense innervation of KP fibers, that is, superior colliculus for visual processing; the inferior colliculus and superior olive for audition; the parabrachial nucleus and nucleus of the solitary tract (NTS or Sol) for gustatory processing; and the olfactory tubercle, nucleus of the olfactory tract, and medial amygdala for olfaction. To our knowledge, the effect of KP on the activity of these regions and on sensory integration has yet to be examined.

4.2 | KP receptor distribution suggests potential autocrine, paracrine, and neurotransmission modes for KP signaling

Our findings highlight the significant expression of the KP receptor (*Kiss1r*) in various brain regions involved in sensory processing and state control, including the main and accessory olfactory bulbs, septal nuclei, tuberomammillary nuclei, suprachiasmatic nucleus, locus coeruleus, hippocampal pyramidal and granule cell layers, thalamic nuclei, cerebellar granule cell layer, and interposed nucleus. Additionally, *Kiss1r* was expressed in *Kiss1*-expressing hypothalamic cells, indicating a potential autocrine/paracrine role for the peptide, as discussed in detail in Section 3.4.

This expression pattern aligns with previous literature that identifies *Kiss1r* in the hippocampus, particularly in the dentate gyrus—an area critical for learning and memory.[32,83] Activation of *Kiss1r* in the hippocampus has been shown to increase the amplitude of excitatory postsynaptic currents (EPSCs), suggesting a potential mechanism by which kisspeptin may enhance synaptic plasticity.[83]

In the habenula, prominent expression of *Kiss1* and *Kiss1r* has been reported,[27,32,33] implicating kisspeptin signaling in emotional regulation, as shown in the zebrafish, where it has been linked to the inhibition of fear responses.[12] Additionally, expressions of *Kiss1r* have been reported in the amygdala, a region pivotal for processing emotions such as fear and anxiety,[27,33] and the septum, which is involved in reward and reinforcement processes.[32] Electrophysiological recordings demonstrate that gonadotropin-releasing hormone (GnRH) septal neurons exhibit robust excitatory responses to kisspeptin application.[84] Moreover, the thalamus, known as a relay center for sensory information, also expresses *Kiss1r*,[27,32] while reports indicate its presence in medullary and pontine brainstem regions.[32,85] *Kiss1r* expression has been reported in the medial amygdala (MeApd) of male rats, contributing to the facilitation of erectile function.[62] Finally, the striatum and cortical regions have also been shown to express *Kiss1r*[27,85] however, we found no studies investigating the potential role of KP signaling in these regions. Collectively, these findings underscore the complex and diverse roles of *Kiss1r* throughout the brain, suggesting that the kisspeptin signaling pathway may be instrumental in modulating a wide array of sensory and emotional processes.

4.3 | Controversies and some consideration of regional KP immunoreactivity as a function of gonadectomy

Rather dramatic down-regulation in mRNA for kisspeptin (*Kiss1*) expression in the RP3V and up-regulation in the Arc region, in terms of dendritic mRNA expression, after acute gonadectomy and a generally stronger *Kiss1* expression in female mice vs. males was recently reported,[1] in agreement with most of the previous reports characterizing KP mRNA expression in this region in both intact and gonadectomized male and female rodents.[86–89] However, altered KP expression at the level of the nerve terminal is more difficult to discern, likely

because immunohistochemical terminal field appearance in a given brain area is determined by the composite projections from multiple KP cell groups, in which KP expression may be variously regulated. In Figure S2, we analyzed the experiments from the Allen Mouse Brain Connectivity Atlas open source to demonstrate the reciprocal and convergent *Kiss1* innervations in the mouse brain of KP^{RP3V} and KP^{Arc} and present these in diagrammatic form in Figure S3.

4.4 | *Mismatches* between KP-ir fiber distribution and *Kiss1r* expression

Mismatches between the chemoanatomical distributions of nerve terminals positive for peptide ligands and their receptors are sometimes seen in various neuropeptidergic systems.[90] Our study shows that KP/*Kiss1r* co-distribution shows some notable discordances of this type. Strong *Kiss1r* expression without corresponding KP-ir fiber appearance is prominent in the MOB, the AOB, the projection neurons of the hippocampal formation, and the granule cell layer of the cerebellum. This "mismatch" has several plausible and biologically relevant explanations. One is the activation of *Kiss1* receptors via KP arriving from anatomically distant sources. We report here densely distributed KP-immunoreactive fibers at the third ventricular wall, with several endings observed at the ventricular lining within the ependymal cell layer (see Section 3.1 of this article and Figure 1A3, E2). This suggests that KP may be released into the ventricular system, allowing it to act at a distance via flow within the cerebrospinal fluid through a humoral-secretory mechanism for KP–KP receptor signaling. A second possibility is that the functional receptor has been axonally transported to a distant location that matches a ligand-releasing site.[91–94] Finally, mismatch may in fact be more apparent than real. The apparent absence of KP-containing axonal projections in regions such as the MOB, AOB, hippocampal formation, and granule layer of the cerebellar cortex may be due to low peptide content in axon projections, in some cases below detectability by immunohistochemical means, and/or the inability of the antibody to recognize all molecular forms of the KP and its metabolites that comprise a family of substances recognized by the receptor.[90] In fact, some of these regions have been reported to receive innervation from regions hosting KP neurons; for instance, the MeA has been shown to innervate the AOB.[95] The ventral premammillary nucleus has been shown to innervate the hippocampal formation and the prefrontal cortex.[96] Some neurons of the nucleus tractus solitarii (NTS) have been shown to send axons to the cerebellar granule cell layer, as well as to the PBN, the Arc, the DMH, and the SHy.[97]

It is our hope that future investigations will be directed toward more functional as well as neuroanatomical analyses of the individual contributions of each KP neuronal population to the nerve terminals within given brain areas.

AUTHOR CONTRIBUTIONS

Limei Zhang: Conceptualization; funding acquisition; investigation; writing – original draft; methodology; validation; visualization; writing – review and editing; formal analysis; project administration; data curation; supervision; resources. **Vito Salvador Hernández:** Conceptualization; investigation; writing – original draft; methodology; validation; visualization; writing – review and editing; formal analysis; data curation. **Mario Alberto Zetter:** Investigation; methodology; validation; visualization; writing – review and editing. **Oscar Rene Hernández-Pérez:** Investigation; writing – review and editing; validation; methodology. **Rafael Hernández-González:** Investigation; writing – original draft; validation; writing – review and editing; resources. **Ignacio Camacho-Arroyo:** Supervision; formal analysis; resources; writing – review and editing; validation. **Lee E. Eiden:** Funding acquisition; writing – original draft; validation; writing – review and editing; project administration; conceptualization; supervision; resources; investigation. **Robert P. Millar:** Conceptualization; resources; writing – review and editing; validation; supervision; funding acquisition.

ACKNOWLEDGMENTS

The research leading to these results received funding from the National Autonomous University of Mexico, under Grant Agreement UNAM-PAPIIT-IG200121(LZ), and UNAM-PAPIIT-IA202724 (ORHP); La Secretaría de Ciencia, Humanidades, Tecnología e Innovación (Secihti) of Mexico, under Grant Agreement CF-2023-243 (LZ), NIMH-IRP, NIH, under Grant Agreement MH002386 (LEE). The investigators of this study have been supported by the following fellowships: sabbatical year fellowship from the PASPA program of the Dirección General de Personal Académico (DGAPA) of the Universidad Nacional Autónoma de México (UNAM) (LZ, VSH); Mexican CONAHCYT sabbatical fellowship (LZ) and Fulbright-García Robles Fellowship (VSH) for a sabbatical research year in LEE's laboratory of NIMH, NIH; DGAPA-UNAM PREI program for a sabbatical research stay (RPM) in LZ's lab in UNAM, Mexico. We thank Charles Gerfen, NIMH, for his support and discussions about this study. We thank Mr. Jonathan Kuo and colleagues of the NIMH-IRP Systems Neuroscience Imaging Resource (SNIR, Director Ted Usdin). Open access funding provided by UNAM.

CONFLICT OF INTEREST

The authors declare no conflicts of interest.

DATA AVAILABILITY STATEMENT

The data that support the findings of this study are available from the corresponding author upon reasonable request.

ORCID

Limei Zhang https://orcid.org/0000-0002-7422-5136
Lee E. Eiden https://orcid.org/0000-0001-7524-944X

REFERENCES

1. Hernández VS, Zetter MA, Hernández-Pérez O, et al. A comprehensive chemotyping, and the gonadal regulation, of seven kisspeptinergic neuronal populations in the mouse brain. *J Neuroendocrinol*. 2025; 37(5):e70019. https://doi.org/10.1111/jne.70019

2. Lee JH, Miele ME, Hicks DJ, et al. KiSS-1, a novel human malignant melanoma metastasis-suppressor gene. *J Natl Cancer Inst*. 1996; 88(23):1731-1737.
3. Pinilla L, Aguilar E, Dieguez C, Millar RP, Tena-Sempere M. Kisspeptins and reproduction: physiological roles and regulatory mechanisms. *Physiol Rev*. 2012;92(3):1235-1316.
4. Clarke H, Dhillo WS, Jayasena CN. Comprehensive review on kisspeptin and its role in reproductive disorders. *Endocrinol Metab*. 2015; 30(2):124-141.
5. Mills EGA, O'Byrne KT, Comninos AN. Kisspeptin as a behavioral hormone. *Semin Reprod Med*. 2019;37(2):56-63.
6. Mills EG, Yang L, Abbara A, Dhillo WS, Comninos AN. Current perspectives on kisspeptins role in behaviour. *Front Endocrinol*. 2022;13: 928143.
7. Stephens SBZ, Kauffman AS. Regulation and possible functions of kisspeptin in the medial amygdala. *Front Endocrinol*. 2017;8:191.
8. Delmas S, Porteous R, Bergin DH, Herbison AE. Altered aspects of anxiety-related behavior in kisspeptin receptor-deleted male mice. *Sci Rep*. 2018;8(1):2794.
9. Ebrahimi Khonacha S, Janahmadi M, Motamedi F. Kisspeptin-13 improves spatial memory consolidation and retrieval against amyloid-beta pathology. *Iran J Pharm Res*. 2019;18(Suppl 1):169-181.
10. Abdul Satar NM, Ogawa S, Parhar IS. Kisspeptin-1 regulates forebrain dopaminergic neurons in the zebrafish. *Sci Rep*. 2020;10(1):19361.
11. Sivalingam M, Ogawa S, Parhar IS. Habenula kisspeptin retrieves morphine impaired fear memory in zebrafish. *Sci Rep*. 2020;10(1):19569.
12. Ogawa S, Nathan FM, Parhar IS. Habenular kisspeptin modulates fear in the zebrafish. *Proc Natl Acad Sci U S A*. 2014;111(10):3841-3846.
13. Liu X, Herbison AE. Kisspeptin regulation of neuronal activity throughout the central nervous system. *Endocrinol Metab*. 2016;31(2): 193-205.
14. Comninos AN, Wall MB, Demetriou L, et al. Kisspeptin modulates sexual and emotional brain processing in humans. *J Clin Invest*. 2017; 127(2):709-719.
15. Clarkson J, d'Anglemont de Tassigny X, Colledge WH, Caraty A, Herbison AE. Distribution of kisspeptin neurones in the adult female mouse brain. *J Neuroendocrinol*. 2009;21(8):673-682.
16. Muir AI, Chamberlain L, Elshourbagy NA, et al. AXOR12, a novel human G protein-coupled receptor, activated by the peptide KiSS-1. *J Biol Chem*. 2001;276(31):28969-28975.
17. Lehman MN, Hileman SM, Goodman RL. Neuroanatomy of the kisspeptin signaling system in mammals: comparative and developmental aspects. *Adv Exp Med Biol*. 2013;784:27-62.
18. Mikkelsen JD, Simonneaux V. The neuroanatomy of the kisspeptin system in the mammalian brain. *Peptides*. 2009;30(1):26-33.
19. Lehman MN, Coolen LM, Steiner RA, et al. The 3(rd) world conference on Kisspeptin, "Kisspeptin 2017: brain and beyond": unresolved questions, challenges and future directions for the field. *J Neuroendocrinol*. 2018;30(5):e12600.
20. Zhang L, Hernandez VS. Synaptic innervation to rat hippocampus by vasopressin-immuno-positive fibres from the hypothalamic supraoptic and paraventricular nuclei. *Neuroscience*. 2013;228:139-162.
21. Swanson LW. *Brain Architecture: Understanding the Basic Plan Oxford*. Oxford University Press; 2011.
22. Lee SH, Dan Y. Neuromodulation of brain states. *Neuron*. 2012;76(1): 209-222.
23. Zagha E, McCormick DA. Neural control of brain state. *Curr Opin Neurobiol*. 2014;29:178-186.
24. Rosazza C, Minati L. Resting-state brain networks: literature review and clinical applications. *Neurol Sci*. 2011;32(5):773-785.
25. McCormick DA, Nestvogel DB, He BJ. Neuromodulation of brain state and behavior. *Annu Rev Neurosci*. 2020;43:391-415.
26. Berridge CW, Waterhouse BD. The locus coeruleus–noradrenergic system: modulation of behavioral state and state-dependent cognitive processes. *Brain Res Rev*. 2003;42(1):33-84.
27. Lee DK, Nguyen T, O'Neill GP, et al. Discovery of a receptor related to the galanin receptors. *FEBS Lett*. 1999;446(1):103-107.
28. Franssen D, Tena-Sempere M. The kisspeptin receptor: a key G-protein-coupled receptor in the control of the reproductive axis. *Best Pract Res Clin Endocrinol Metab*. 2018;32(2):107-123.
29. Irwig MS, Fraley GS, Smith JT, et al. Kisspeptin activation of gonadotropin releasing hormone neurons and regulation of KiSS-1 mRNA in the male rat. *Neuroendocrinology*. 2004;80(4):264-272.
30. Ringel MD, Hardy E, Bernet VJ, et al. Metastin receptor is overexpressed in papillary thyroid cancer and activates MAP kinase in thyroid cancer cells. *J Clin Endocrinol Metab*. 2002;87(5):2399.
31. Wu Z, Chen G, Qiu C, et al. Structural basis for the ligand recognition and G protein subtype selectivity of kisspeptin receptor. *Sci Adv*. 2024;10(33):eadn7771.
32. Herbison AE, de Tassigny X, Doran J, Colledge WH. Distribution and postnatal development of Gpr54 gene expression in mouse brain and gonadotropin-releasing hormone neurons. *Endocrinology*. 2010; 151(1):312-321.
33. Higo S, Honda S, Iijima N, Ozawa H. Mapping of kisspeptin receptor mRNA in the whole rat brain and its co-localisation with oxytocin in the paraventricular nucleus. *J Neuroendocrinol*. 2016;28(4):2-8.
34. Stout Steele M, Bennett RA. Clinical technique: dorsal ovariectomy in rodents. *J Exotic Pet Med*. 2011;20(3):222-226.
35. Sophocleous A, Idris AI. Ovariectomy/orchiectomy in rodents. In: Idris AI, ed. *Bone Research Protocols*. Springer New York; 2019: 261-267.
36. Dhillo WS, Chaudhri OB, Patterson M, et al. Kisspeptin-54 stimulates the hypothalamic-pituitary gonadal axis in human males. *J Clin Endocrinol Metab*. 2005;90(12):6609-6615.
37. Paxinos G, Franklin KBJ. *Paxinos and Franklin's the Mouse Brain in Stereotaxic Coordinates*. Elsevier Science; 2012.
38. Paxinos G, Watson C. *The Rat Brain in Stereotaxic Coordinates*. Elsevier Science; 2007.
39. Zhang L, Hernandez VS, Gerfen CR, et al. Behavioral role of PACAP signaling reflects its selective distribution in glutamatergic and GABAergic neuronal subpopulations. *Elife*. 2021;10:e61718.
40. Zhang L, Hernandez VS, Zetter MA, Eiden LE. VGLUT-VGAT expression delineates functionally specialised populations of vasopressin-containing neurones including a glutamatergic perforant path-projecting cell group to the hippocampus in rat and mouse brain. *J Neuroendocrinol*. 2020;32(4):e12831.
41. Brailoiu GC, Dun SL, Ohsawa M, et al. KiSS-1 expression and metastin-like immunoreactivity in the rat brain. *J Comp Neurol*. 2005; 481(3):314-329.
42. Ketterson ED, Nolan V. Adaptation, exaptation, and constraint: a hormonal perspective. *Am Nat*. 1999;154(S1):S4-S25.
43. Risold PY, Swanson LW. Connections of the rat lateral septal complex. *Brain Res Brain Res Rev*. 1997;24(2–3):115-195.
44. Rizzi-Wise CA, Wang DV. Putting together pieces of the lateral septum: multifaceted functions and its neural pathways. *eNeuro*. 2021;8(6):2-11.
45. Sheehan TP, Chambers RA, Russell DS. Regulation of affect by the lateral septum: implications for neuropsychiatry. *Brain Res Brain Res Rev*. 2004;46(1):71-117.
46. Salib M, Joshi A, Katona L, et al. GABAergic medial septal neurons with low-rhythmic firing innervating the dentate gyrus and hippocampal area CA3. *J Neurosci*. 2019;39(23):4527-4549.
47. Unal G, Crump MG, Viney TJ, et al. Spatio-temporal specialization of GABAergic septo-hippocampal neurons for rhythmic network activity. *Brain Struct Funct*. 2018;223(5):2409-2432.
48. Buzsaki G. Theta oscillations in the hippocampus. *Neuron*. 2002;33(3): 325-340.
49. Espinosa N, Alonso A, Caneo M, Moran C, Fuentealba P. Optogenetic suppression of lateral septum somatostatin neurons enhances hippocampus cholinergic theta oscillations and local synchrony. *Brain Sci*. 2022;13(1):1.

50. Shen L, Zhang GW, Tao C, et al. A bottom-up reward pathway mediated by somatostatin neurons in the medial septum complex underlying appetitive learning. *Nat Commun*. 2022;13(1):1194.
51. Srividya R, Mallick HN, Kumar VM. The changes in thermal preference, sleep-wakefulness, body temperature and locomotor activity in the rats with medial septal lesion. *Behav Brain Res*. 2005;164(2):147-155.
52. Tsanov M. Speed and oscillations: medial septum integration of attention and navigation. *Front Syst Neurosci*. 2017;11:67.
53. Joshi A, Salib M, Viney TJ, Dupret D, Somogyi P. Behavior-dependent activity and synaptic organization of septo-hippocampal GABAergic neurons selectively targeting the hippocampal CA3 area. *Neuron*. 2017;96(6):1342-1357.
54. Liu AKL, Lim EJ, Ahmed I, Chang RC, Pearce RKB, Gentleman SM. Review: revisiting the human cholinergic nucleus of the diagonal band of Broca. *Neuropathol Appl Neurobiol*. 2018;44(7):647-662.
55. Dudek SM, Alexander GM, Farris S. Rediscovering area CA2: unique properties and functions. *Nat Rev Neurosci*. 2016;17(2):89-102.
56. Semba K, Fibiger HC. Organization of central cholinergic systems. *Prog Brain Res*. 1989;79:37-63.
57. Floresco SB. The nucleus accumbens: an interface between cognition, emotion, and action. *Annu Rev Psychol*. 2015;66:25-52.
58. Riaz S, Puveendrakumaran P, Khan D, Yoon S, Hamel L, Ito R. Prelimbic and infralimbic cortical inactivations attenuate contextually driven discriminative responding for reward. *Sci Rep*. 2019;9(1):3982.
59. Capuzzo G, Floresco SB. Prelimbic and infralimbic prefrontal regulation of active and inhibitory avoidance and reward-seeking. *J Neurosci*. 2020;40(24):4773-4787.
60. de Lima MAX, Baldo MVC, Oliveira FA, Canteras NS. The anterior cingulate cortex and its role in controlling contextual fear memory to predatory threats. *Elife*. 2022;11:e67007.
61. Kataoka N, Shima Y, Nakajima K, Nakamura K. A central master driver of psychosocial stress responses in the rat. *Science*. 2020;367(6482):1105-1112.
62. Gresham R, Li S, Adekunbi DA, Hu M, Li XF, O'Byrne KT. Kisspeptin in the medial amygdala and sexual behavior in male rats. *Neurosci Lett*. 2016;627:13-17.
63. Pineda R, Plaisier F, Millar RP, Ludwig M. Amygdala kisspeptin neurons: putative mediators of olfactory control of the gonadotropic axis. *Neuroendocrinology*. 2017;104(3):223-238.
64. Kim J, Semaan SJ, Clifton DK, Steiner RA, Dhamija S, Kauffman AS. Regulation of Kiss1 expression by sex steroids in the amygdala of the rat and mouse. *Endocrinology*. 2011;152(5):2020-2030.
65. Dubois SL, Acosta-Martinez M, DeJoseph MR, et al. Positive, but not negative feedback actions of estradiol in adult female mice require estrogen receptor alpha in kisspeptin neurons. *Endocrinology*. 2015;156(3):1111-1120.
66. Rance NE. Menopause and the human hypothalamus: evidence for the role of kisspeptin/neurokinin B neurons in the regulation of estrogen negative feedback. *Peptides*. 2009;30(1):111-122.
67. Starrett JR, Moenter SM. Hypothalamic kisspeptin neurons as potential mediators of estradiol negative and positive feedback. *Peptides*. 2023;163:170963.
68. Daikoku S, Tsuruo Y, Hashimoto T, Okamura Y, Yokote R, Ide M. Hypothalamic neurons from a developmental aspect. *Arch Histol Cytol*. 1989;52(Suppl 2):17-23.
69. Bailey DJ, Saldanha CJ. The importance of neural aromatization in the acquisition, recall, and integration of song and spatial memories in passerines. *Horm Behav*. 2015;74:116-124.
70. Goodman RL, Moore AM, Onslow K, et al. Lesions of KNDy and Kiss1R neurons in the arcuate nucleus produce different effects on LH pulse patterns in female sheep. *Endocrinology*. 2023;164(11):1-19.
71. Kim TH, Yoon JH, Cho SG. Kisspeptin promotes glioblastoma cell invasiveness via the Gq-PLC-PKC pathway. *Anticancer Res*. 2020;40(1):213-220.
72. Sinen O, Sinen AG, Derin N, Aslan MA. Nasal application of kisspeptin-54 mitigates motor deficits by reducing nigrostriatal dopamine loss in hemiparkinsonian rats. *Behav Brain Res*. 2024;468:115035.
73. Klinger K, Del Angel M, Caliskan G, Stork O. Increasing NPYergic transmission in the hippocampus rescues aging-related deficits of long-term potentiation in the mouse dentate gyrus. *Front Aging Neurosci*. 2023;15:1283581.
74. Reglodi D, Atlasz T, Szabo E, et al. PACAP deficiency as a model of aging. *Geroscience*. 2018;40(5–6):437-452.
75. Kappeler L, Gourdji D, Zizzari P, Bluet-Pajot MT, Epelbaum J. Age-associated changes in hypothalamic and pituitary neuroendocrine gene expression in the rat. *J Neuroendocrinol*. 2003;15(6):592-601.
76. Kunimura Y, Iwata K, Ishigami A, Ozawa H. Age-related alterations in hypothalamic kisspeptin, neurokinin B, and dynorphin neurons and in pulsatile LH release in female and male rats. *Neurobiol Aging*. 2017;50:30-38.
77. Rometo AM, Krajewski SJ, Voytko ML, Rance NE. Hypertrophy and increased kisspeptin gene expression in the hypothalamic infundibular nucleus of postmenopausal women and ovariectomized monkeys. *J Clin Endocrinol Metab*. 2007;92(7):2744-2750.
78. Biesbroek JM, Verhagen MG, van der Stigchel S, Biessels GJ. When the central integrator disintegrates: a review of the role of the thalamus in cognition and dementia. *Alzheimers Dement*. 2024;20(3):2209-2222.
79. Ogawa S, Parhar IS. Functions of habenula in reproduction and socio-reproductive behaviours. *Front Neuroendocrinol*. 2022;64:100964.
80. Stincic TL, Qiu J, Connors AM, Kelly MJ, Ronnekleiv OK. Arcuate and preoptic kisspeptin neurons exhibit differential projections to hypothalamic nuclei and exert opposite postsynaptic effects on hypothalamic paraventricular and dorsomedial nuclei in the female mouse. *eNeuro*. 2021;8(4):1-26.
81. Csabafi K, Jaszberenyi M, Bagosi Z, Liptak N, Telegdy G. Effects of kisspeptin-13 on the hypothalamic-pituitary-adrenal axis, thermoregulation, anxiety and locomotor activity in rats. *Behav Brain Res*. 2013;241:56-61.
82. Kelestimur H, Bulut F, Canpolat S, Ozcan M, Ayar A. Kisspeptin leads to calcium signaling in cultured rat dorsal root ganglion neurons. *Gen Physiol Biophys*. 2021;40(2):155-160.
83. Arai AC. The role of kisspeptin and GPR54 in the hippocampus. *Peptides*. 2009;30(1):16-25.
84. Dumalska I, Wu M, Morozova E, Liu R, van den Pol A, Alreja M. Excitatory effects of the puberty-initiating peptide kisspeptin and group I metabotropic glutamate receptor agonists differentiate two distinct subpopulations of gonadotropin-releasing hormone neurons. *J Neurosci*. 2008;28(32):8003-8013.
85. Mattam U, Talari NK, Thiriveedi VR, et al. Aging reduces kisspeptin receptor (GPR54) expression levels in the hypothalamus and extra-hypothalamic brain regions. *Exp Ther Med*. 2021;22(3):1019.
86. Smith JT, Cunningham MJ, Rissman EF, Clifton DK, Steiner RA. Regulation of Kiss1 gene expression in the brain of the female mouse. *Endocrinology*. 2005;146(9):3686-3692.
87. Smith JT, Dungan HM, Stoll EA, et al. Differential regulation of KiSS-1 mRNA expression by sex steroids in the brain of the male mouse. *Endocrinology*. 2005;146(7):2976-2984.
88. Kauffman AS. Gonadal and nongonadal regulation of sex differences in hypothalamic Kiss1 neurones. *J Neuroendocrinol*. 2010;22(7):682-691.
89. Takumi K, Iijima N, Iwata K, Higo S, Ozawa H. The effects of gonadal steroid manipulation on the expression of Kiss1 mRNA in rat arcuate nucleus during postnatal development. *J Physiol Sci*. 2012;62(6):453-460.
90. Herkenham M. Mismatches between neurotransmitter and receptor localizations in brain: observations and implications. *Neuroscience*. 1987;23(1):1-38.

91. Miller RJ. Presynaptic receptors. *Annu Rev Pharmacol Toxicol*. 1998; 38:201-227.
92. Colmers WF, Lukowiak K, Pittman QJ. Neuropeptide Y action in the rat hippocampal slice: site and mechanism of presynaptic inhibition. *J Neurosci*. 1988;8(10):3827-3837.
93. van den Pol AN, Gao XB, Obrietan K, Kilduff TS, Belousov AB. Presynaptic and postsynaptic actions and modulation of neuroendocrine neurons by a new hypothalamic peptide, hypocretin/orexin. *J Neurosci*. 1998;18(19):7962-7971.
94. Lopez-Huerta VG, Blanco-Hernandez E, Bargas J, Galarraga E. Presynaptic modulation by somatostatin in the rat neostriatum is altered in a model of parkinsonism. *J Neurophysiol*. 2012;108(4):1032-1043.
95. Mori K, Sakano H. Olfactory circuitry and behavioral decisions. *Annu Rev Physiol*. 2021;83:231-256.
96. Canteras NS, Simerly RB, Swanson LW. Projections of the ventral premammillary nucleus. *J Comp Neurol*. 1992;324(2):195-212.
97. Zhu M, Jun S, Nie X, et al. Mapping of afferent and efferent connections of phenylethanolamine N-methyltransferase-expressing neurons in the nucleus tractus solitarii. *CNS Neurosci Ther*. 2024; 30(6):e14808.

SUPPORTING INFORMATION

Additional supporting information can be found online in the Supporting Information section at the end of this article.

How to cite this article: Zhang L, Hernández VS, Zetter MA, et al. Kisspeptin fiber and receptor distribution analysis suggests its potential role in central sensorial processing and behavioral state control. *J Neuroendocrinol*. 2025;37(5): e70007. doi:10.1111/jne.70007